A potential role for α-actinin in inside-out αIIbβ3 signaling

Seiji Tadokoro,[1,2] Tsuyoshi Nakazawa,[1] Tsuyoshi Kamae,[1] Kazunobu Kiyomizu,[1] Hirokazu Kashiwagi,[1] Shigenori Honda,[3] Yuzuru Kanakura,[1] and Yoshiaki Tomiyama[1,2]

[1]Department of Hematology and Oncology, Osaka University Graduate School of Medicine C9, Osaka, Japan; [2]Department of Blood Transfusion, Osaka University Hospital, Osaka, Japan; and [3]National Cardiovascular Center Research Institute, Osaka, Japan

Many different biochemical signaling pathways regulate integrin activation through the integrin cytoplasmic tail. Here, we describe a new role for α-actinin in inside-out integrin activation. In resting human platelets, α-actinin was associated with αIIbβ3, whereas inside-out signaling (αIIbβ3 activation signals) from protease-activated receptors (PARs) dephosphorylated and dissociated α-actinin from αIIbβ3. We evaluated the time-dependent changes of the αIIbβ3 activation state by measuring PAC-1 binding velocity. The initial velocity analysis clearly showed that PAR1-activating peptide stimulation induced only transient αIIbβ3 activation, whereas PAR4-activating peptide induced long-lasting αIIbβ3 activation. When αIIbβ3 activation signaling dwindled, α-actinin became rephosphorylated and reassociated with αIIbβ3. Compared with control platelets, the dissociation of α-actinin from αIIbβ3 was only transient in PAR4-stimulated $P2Y_{12}$-deficient platelets in which the sustained αIIbβ3 activation was markedly impaired. Overexpression of wild-type α-actinin, but not the mutant Y12F α-actinin, increased its binding to αIIbβ3 and inhibited PAR1-induced initial αIIbβ3 activation in the human megakaryoblastic cell line, CMK. In contrast, knockdown of α-actinin augmented PAR-induced αIIbβ3 activation in CMK. These observations suggest that α-actinin might play a potential role in setting integrins to a default low-affinity ligand-binding state in resting platelets and regulating αIIbβ3 activation by inside-out signaling. (*Blood.* 2011;117(1):250-258)

Introduction

Integrins and their ligands play key roles in development, immune responses, leukocyte traffic, hemostasis, and cancer and are at the core of numerous human diseases.[1] Many integrins are expressed with their extracellular domains in a default low-affinity ligand-binding state. The main platelet integrin, αIIbβ3, also known as GPIIb/IIIa, is present at a high density on circulating platelets. It is inactive on circulating platelets; if it were not, platelets would bind their main ligand, fibrinogen, from the plasma and aggregate, leading to thrombosis. This inactivation is important for the biologic function of integrins, as is most evident from assessments of their status on circulating blood cells. However, the molecular mechanisms of their being set to an inactive, low-affinity state remain unknown.

High-affinity ligand binding requires activation of integrins through conformational changes regulated by inside-out signaling.[2] Integrin cytoplasmic domains play a pivotal role in integrin signaling because the cytoplasmic tails of the integrin α and β subunits are directly accessible to the intracellular signaling apparatus, namely the integrin activation complex (IAC).[3] Moreover, ligand binding to the integrin induces outside-in signaling that leads to integrin clustering and subsequent recruitment of actin filaments to the integrin cytoplasmic domain. From the perspective that this recruitment occurs by a complex of interacting cytoskeletal proteins, many studies have focused on the components of the IAC, including talin, kindlin, filamin, and α-actinin. The binding of talin to the integrin β subunit cytoplasmic tail is a common final step in the activation process.[4-8] Kindlins bind to the more C-terminal of the NPxY motifs in β-integrin tails and modulate integrin activation.[9-11] Filamin binding to β integrin cytoplasmic tails is competitive with that of talin.[12] Although these studies suggest a model in which multiple proteins jockey for position on the β integrin tail, how cells orchestrate the process remains less well understood.

α-Actinin plays multiple important roles in the cell.[13,14] It links the cytoskeleton to different transmembrane proteins in a variety of junctions, regulates activity of several receptors, and serves as a scaffold connecting the cytoskeleton to diverse signaling pathways. α-Actinin binds to the β integrin cytoplasmic tail,[15,16] and recent studies have shown that the interaction between α-actinin and the integrin β2 tail modulates integrin affinity.[17,18] For regulating α-actinin function, 4 main mechanisms have been identified to date: processing by proteases, binding to phosphatidylinositol intermediaries, phosphorylation by tyrosine kinases, and binding to calcium. For tyrosine phosphorylation regulation, a second wave of protein tyrosine phosphorylation that is strictly dependent on both ligand binding to αIIbβ3 and cytoskeleton organization was observed in platelets stimulated by thrombin, phorbol myristate acetate, or immobilized fibrinogen.[19] Platelet adhesion and spreading on fibrinogen, mediated by the integrin αIIbβ3, trigger a robust and sustained phosphorylation of focal adhesion kinase and α-actinin by outside-in signaling.[20,21] Focal adhesion kinase phosphorylates α-actinin, which lowers its affinity for actin.[22] Dephosphorylation of α-actinin is regulated by the protein tyrosine phosphatase (PTP) SHP-1 (also named PTP1C, SHPTP-1, SHP,

Submitted October 6, 2009; accepted October 1, 2010. Prepublished online as *Blood* First Edition paper, October 12, 2010; DOI 10.1182/blood-2009-10-246751.

The online version of this article contains a data supplement.

The publication costs of this article were defrayed in part by page charge payment. Therefore, and solely to indicate this fact, this article is hereby marked "advertisement" in accordance with 18 USC section 1734.

HCP, and PTPN6),[23] a main PTP expressed in platelets. Although the regulation of α-actinin by outside-in signaling has been well characterized, its role in inside-out signaling remains to be determined.

Here, we show that α-actinin is associated with resting αIIbβ3 in platelets. Inside-out signaling from thrombin receptors, protease-activated receptor 1 (PAR1) and PAR4, dephosphorylated and dissociated α-actinin from αIIbβ3. Protease-activated receptor 1–activating peptide (PAR1-AP) and PAR4-AP induce transient and sustained αIIbβ3 activation, respectively. When the αIIbβ3 activation signaling dwindled, α-actinin reassociated with αIIbβ3 on rephosphorylation. Our observations suggest an emergent picture of α-actinin as having a role in keeping integrins in a default low-affinity ligand-binding state and regulating integrin activation.

Methods

Preparation of human platelets

Platelets were taken from healthy donors as approved by the institutional review board of Osaka University and were prepared as described previously[24] with some modifications. In brief, venous blood was obtained from volunteers with acid citrate dextrose solution (National Institute of Health formula A) as an anticoagulant, used at a 1:6 vol/vol ratio. Platelet-rich plasma was obtained by centrifugation at 250*g* for 10 minutes. After incubation with 0.5μM prostaglandin E_1 for 15 minutes, platelets were isolated by centrifugation of the platelet-rich plasma at 750*g* for 10 minutes. The pellet was washed twice with PIPES (Piperazine-1,4-bis(2-ethanesulfonic acid)) saline buffer (0.15M NaCl, 20mM PIPES, pH 6.5). The washed platelets were resuspended in Walsh buffer (137mM NaCl, 2.7mM KCl, 1mM $MgCl_2$, 3.3mM NaH_2PO4, 3.8mM HEPES [N-2-hydroxyethylpiperazine-N′-2-ethanesulfonic acid], 0.1% glucose, 0.1% bovine serum albumin [BSA], pH 7.4) to a density of 4×10^8 platelets/mL and allowed to sit for 30 minutes before use.

Antibodies

The monoclonal anti–α-actinin antibody (BM-75.2) and anti–talin antibody (8d4) were purchased from Sigma-Aldrich. The monoclonal anti–α-actinin antibody (H-2) and horseradish peroxidase (HRP)–conjugated anti–mouse immunoglobulin M (IgM) were purchased from Santa Cruz Biotechnology. Anti–vasodilator-stimulated phosphoprotein (VASP) monoclonal antibody (IE273) was purchased from ImmunoGlobe. The antiphosphotyrosine (4G10) antibody and anti–phospho-VASP-Ser239 (16C2) were purchased from Upstate Cell Signaling Solutions. PAC-1, the monoclonal, ligand-mimetic, αIIbβ3-specific antibody that binds specifically to activated αIIbβ3, the allophycocyanin-conjugated monoclonal anti-CD25 antibody, allophycocyanin-conjugated anti-CD42b antibody, and phycoerythrin-conjugated anti-CD42b antibody were purchased from BD Biosciences. peridinin chlorophyll protein complex–cyanine 5.5 (PerCP-Cy5.5)–conjugated anti-CD25 antibody was purchased from eBioscience. The polyclonal anti-αIIbβ3 antibody was a gift from Dr Thomas J. Kunicki (The Scripps Research Institute), and the monoclonal anti-αIIbβ3 antibody that activates αIIbβ3, PT25-2,[25] was a gift from Drs. Makoto Handa and Yasuo Ikeda (Keio University). HRP-conjugated secondary antibodies, anti–mouse IgG (H+L), and anti–rabbit IgG (H+L) were purchased from Cell Signaling Technology. Fluorescein isothiocyanate (FITC)– or phycoerythrin-conjugated anti–mouse IgM (μ) was purchased from Caltag Laboratories.

Chemicals

PAR1-AP (SFLLRN), thrombin, and prostaglandin E_1 were purchased from Sigma-Aldrich. PAR4-AP (AYPGKF) was purchased from GenixTalk. AR-C69931MX, a $P2Y_{12}$-specific antagonist, was a gift from Astra-Zeneca. FK633, an αIIbβ3-specific antagonist,[26] was a gift from Astellas Pharma Inc. Protein phosphatase inhibitor-1 (PTPI-1) was purchased from Calbiochem.

Immunoprecipitation

Aliquots of washed platelets (4×10^8/mL) were incubated with PAR1-AP (25μM), PAR4-AP (150μM), or thrombin (0.2 U/mL) at room temperature. Reactions were stopped by lysis of platelets with an equal volume of 2 × neutral detergent lysis buffer (15mM HEPES, 150mM NaCl, 2% [vol/vol] Triton X-100, 10mM EGTA [ethylene glycol tetraacetic acid], and 1mM Na_3VO_4, pH 7.4, plus complete protease inhibitors purchased from Roche Applied Science). Insoluble debris was cleared from the lysate by centrifugation at 13 000*g* for 4 minutes at 4°C. Supernatants were precleared with protein G-sepharose (GE Healthcare) for 1 hour. Precleared lysates were added to the newly prepared protein G with 1 μg of antibody and incubated at 4°C with constant rotation. Immunoprecipitates were washed 3 times, and proteins were eluted from the beads by incubation of the immunoprecipitates with 20 μL of 3 × sodium dodecylsulfate (SDS) sample buffer (62.5mM Tris [tris(hydroxymethyl)aminomethane], pH 6.8, 25% [vol/vol] glycerol, 2% [vol/vol] SDS, 5mM 2-mercaptoethanol, and 0.01% bromophenol blue) at 96°C for 5 minutes.

Electrophoresis of proteins and immunoblotting

Proteins were separated by continuous SDS–polyacrylamide gel electrophoresis on 4%-20% gels and electrophoretically transferred to Immobilon-P phenylmethlsulfonyl fluoride membranes (Millipore). Membranes were blocked by incubation with 2% (wt/vol) BSA in TBST (150mM NaCl, 50mM Tris, and 0.1% [vol/vol] Tween 20, pH 7.4). Primary antibodies were diluted in 2% (wt/vol) BSA in TBST. After incubation with primary antibodies, membranes were washed with TBST and incubated with HRP-conjugated secondary antibodies for 1 hour at room temperature. After further washing of the membrane, signals were detected by enhanced chemiluminescence. When necessary, membranes were immersed in Restore Western blot stripping buffer (Pierce Chemical) and incubated at room temperature for 30 minutes before extensive washing and reprobing with the appropriate antibody.

Cell culture, plasmids, and transfections

Mammalian expression plasmids, including pcDNA/α-actinin, were a gift from Dr Beatrice Haimovich (University of Medicine and Dentistry of New Jersey). The mutant α-actinin carrying a phenylalanine at position 12 (Y12F) was generated as described.[22] CMK cells were maintained in culture as described previously.[27] Ribavirin was not used in this study. The plasmid encoding the extracellular and transmembrane domains of the Tac subunit of the human interleukin-2 receptor was generated as described.[28] Nucleofection was performed with Nucleofector II (Amaxa Biosystems) according to the manufacturer's instructions. CMK cells were nucleofected with 10 μg/cuvette Tac subunit of the human interleukin-2 receptor–encoding plasmid and 20 μg/cuvette α-actinin–encoding plasmid. Cells were analyzed 20 hours after nucleofection. The short hairpin RNAs (shRNAs) lentiviral particules were generated as described.[4] 5′-GGAAGCCAGGCATGTGGTTCTGATCATTGG AAGCTTGCGATGATTAGGACTACATGCCTGTCTTCCTTTTTT-3′ and 5′-GGCCAGCTTCTCGTAGTCTTCCATAAGCTGAAGCTT GAGCTTATGGAGGATTATGAGAAGCTGGCTTTTTTT-3′ oligonucleotide sequences were used to construct control and α-actinin shRNA, respectively. The α-actinin shRNA sequence chosen is specific for human α-actinin-1 and is 82% conserved in the human α-actinin-4 nucleotide sequence. shRNA viral vectors were produced by cloning the siRNA cassette into the FG12 lentiviral transgene vector in which DsRed2 was substituted for enhanced green fluorescent protein. In plasmids encoding wild-type or mutant α-actinin, 3 silence mutations were generated to prevent annealing with the α-actinin shRNA.

Flow cytometry and platelet aggregometry

Aliquots of washed platelets and FITC–PAC-1 were incubated with PAR1-AP (25μM), PAR4-AP (150μM), or thrombin (0.2 U/mL) at room temperature for various times. Binding of PAC-1 to platelets or CMK cells was assessed by flow cytometry with the use of FACSCalibur (Becton Dickinson).[29] The initial velocity of bound PAC-1 was analyzed as

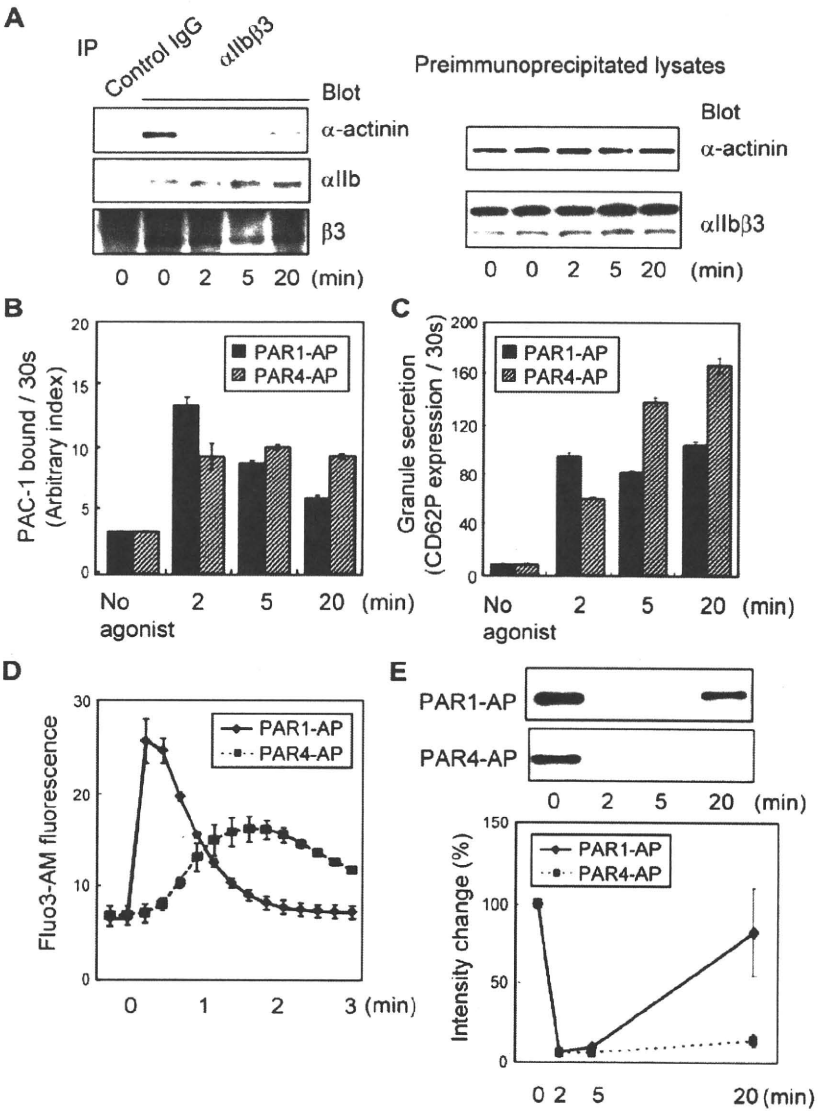

Figure 1. Dynamic changes in the interaction between αIIbβ3 and α-actinin in platelets. Washed human platelets were stimulated with PAR1-AP (25μM) or PAR4-AP (150μM) under nonstirring conditions for the time indicated. (A) αIIbβ3 was immunoprecipitated from lysates prepared from human platelets stimulated with PAR1-AP. Immunoprecipitates were then subjected to SDS–polyacrylamide gel electrophoresis (PAGE) and immunoblotted with anti–α-actinin antibody. Immunoblots were stripped and reprobed with anti-αIIbβ3 antibody. Preimmunoprecipitated lysates were also subjected to SDS-PAGE and immunoblotted with the same series of antibodies. (B) FITC–PAC-1 was added to the activated platelets after stimulation and incubated for 30 seconds to obtain the PAC-1 binding velocity at the time indicated. PAC-1 binding/30 seconds was normalized for integrin expression levels. (C) Phycoerythrin-conjugated anti-CD62P was added to the activated platelets and incubated for only 30 seconds to evaluate granule secretion. (D) Intracellular calcium mobilization was assessed by monitoring Fluo3-AM fluorescence by flow cytometry. (E) αIIbβ3 was immunoprecipitated then immunoblotted with anti–α-actinin antibody. Immunoblots shown are representative of 3 different experiments and analyzed by scanning densitometry and quantified with ImageJ (National Institutes of Health).

described.[30] In brief, washed platelets were mixed with PAR-AP at time "zero." At different time points from 2 minutes to 20 minutes, 20 μL of FITC–PAC-1 was added, and 30 seconds after the addition of PAC-1, 50 μL of platelet suspension was diluted into Walsh buffer, and bound PAC-1 was measured by flow cytometry. PAR1-AP–induced PAC-1 binding to CMK cells was analyzed on a gated subset of live (propidium iodide negative) differentiated (strongly $CD42b^+$) transfected (strongly $CD25^+$ or $DsRed2^+$) cells. Specific binding was assessed as total binding minus binding in the presence of 10μM FK633. Intracellular α-actinin expression was assessed by flow cytometry as previously described.[4] In brief, CMK cells were fixed with 0.5% paraformaldehyde, permeabilized with 0.05% saponin, and incubated for 30 minutes at room temperature with anti–α-actinin monoclonal antibody. After washing, the cells were incubated another 30 minutes with FITC-conjugated goat anti–mouse IgM. Cells were washed and resuspended in 500 μL of phosphate-buffered saline then analyzed by flow cytometry.

Presentation of data

Data are presented as mean ± SEM of ≥ 3 individual experiments from different blood donors. Analysis of statistical significance was performed with Student paired *t* tests, and differences were considered significant when $P < .05$. Immunoblots shown are representatives of 3 different experiments and were analyzed by scanning densitometry and quantified with ImageJ Version 1.40g (National Institutes of Health).

Results

Dynamic changes in the interaction between αIIbβ3 and α-actinin in platelets

Human washed platelets were stimulated with 25μM PAR1-AP under nonstirring conditions for ≤ 20 minutes to explore the role of α-actinin in inside-out signaling. Immunoprecipitation with polyclonal anti-αIIbβ3 followed by immunoblotting with anti–α-actinin showed that, in resting platelets, α-actinin was already associated with resting αIIbβ3 (Figure 1A). When platelets were stimulated with PAR1-AP, α-actinin was dissociated from αIIbβ3. Some actin-binding proteins moved to the Triton X-100–insoluble

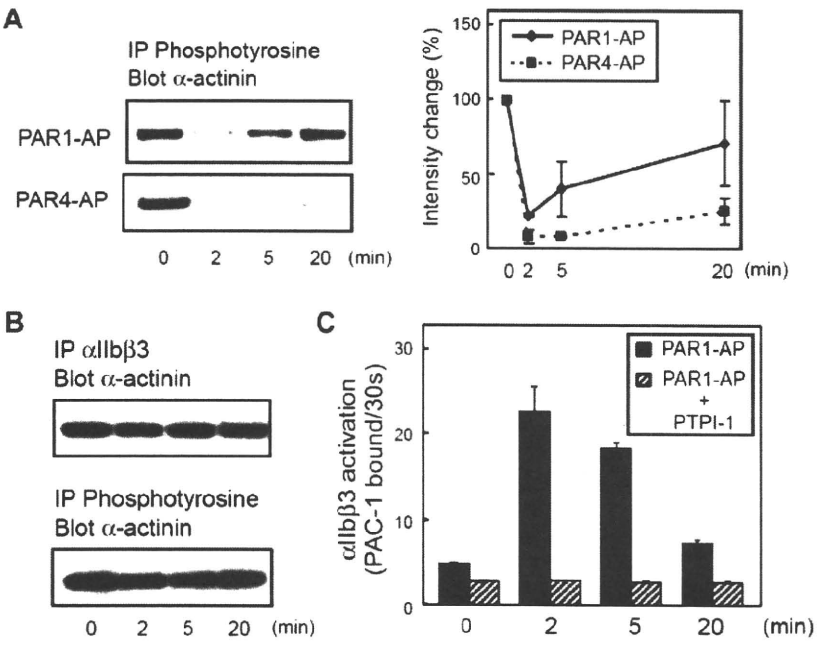

Figure 2. Kinetics of tyrosine phosphorylation of α-actinin during platelet activation and inhibition of SHP-1 by PTPI-1. Washed human platelets were stimulated with PAR1-AP (25μM) or PAR4-AP (150μM) for the time indicated. (A) Tyrosine-phosphorylated proteins were immunoprecipitated then immunoblotted with anti–α-actinin antibody. Immunoblots were analyzed by scanning densitometry and were quantified with ImageJ. (B) Washed human platelets were incubated at room temperature for 2 minutes in the presence of PTPI-1 (50μM). The platelets were then stimulated with PAR1-AP (25μM) for the time indicated. αIIbβ3 or tyrosine-phosphorylated proteins were immunoprecipitated then immunoblotted with anti–α-actinin antibody. (C) FITC–PAC-1 was added to the activated platelets after stimulation and incubated for 30 seconds to obtain the PAC-1 binding velocity at the time indicated. Error bars represent SEMs of 3 experiments.

fraction from the Triton X-100–soluble fraction in response to platelet activation; however, the amounts of α-actinin, talin, and αIIbβ3 in the Triton X-100–soluble fraction of PAR1-AP–activated platelets were similar to those of resting platelets under our experimental conditions. This finding suggests that the dissociation was not the result of the translocation of α-actinin into the Triton X-100–insoluble fraction. This dissociation remained unaffected even in the presence of 10μM of the αIIbβ3-specific peptidomimetic antagonist FK633, suggesting that the dissociation is independent of αIIbβ3-mediated outside-in signaling (data not shown). Interestingly, α-actinin rebound to αIIbβ3 at 20 minutes after PAR1-AP stimulation.

To clarify the physiologic relevance of the α-actinin dissociation to αIIbβ3 activation, we measured the amounts of PAC-1 binding after PAR1-AP or PAR4-AP stimulation. FITC–PAC-1 was incubated with activated platelets for 2 minutes, 5 minutes, and 20 minutes. Under PAR4-AP stimulation, the levels of PAC-1 binding increased as the incubation time extended. However, with PAR1-AP stimulation, the level of PAC-1 binding for a 20-minute incubation was similar to (or even lower than) that for a 5-minute incubation, suggesting that the number of activated αIIbβ3 molecules decreased at 20 minutes after PAR1-AP stimulation (supplemental Figure 1A, available on the *Blood* Web site; see the Supplemental Materials link at the top of the online article).

To evaluate more precisely the dynamic changes in the αIIbβ3 activation state, we performed initial velocity analysis for PAC-1 binding that has recently been developed.[30] In brief, FITC–PAC-1 was added to the activated platelets at the indicated time points after stimulation and incubated for only 30 seconds to obtain the PAC-1 binding velocity at the time points in question. The velocity of PAC-1 binding reflects the relative numbers of activated αIIbβ3 at those time points. PAC-1 binding was normalized for integrin expression levels. This initial velocity analysis clearly showed that PAR1 stimulation induced only transient αIIbβ3 activation, whereas PAR4 induced long-lasting αIIbβ3 activation (Figure 1B). Moreover, we assessed granule secretion and calcium mobilization under these conditions. These agonists induced different kinetics in CD62P expression and intracellular calcium mobilization, as detected by Fluo3-AM fluorescence (Figure 1C-D). These characteristics are consistent with the observed transient and sustained αIIbβ3 activation induced by PAR1-AP and PAR4-AP, respectively (Figure 1E). These data suggest that the dissociation of α-actinin may be related to αIIbβ3 activation.

Tyrosine phosphorylation of α-actinin regulates the interaction between α-actinin and αIIbβ3 in platelets

Because the α-actinin function appears to be regulated, in part, by tyrosine phosphorylation, we then examined the tyrosine phosphorylation state of α-actinin. The tyrosine-phosphorylated α-actinin was detectable as a faint band by immunoprecipitation with α-actinin antibody (BM-75.2 or H-2) followed by immunoblotting with 4G10 (supplemental Figure 1B). Accordingly, we modified our methods, and the platelet lysate was first subjected to immunoprecipitation with monoclonal antibody 4G10, followed by immunoblotting with anti–α-actinin antibody. In resting platelets, the anti–α-actinin antibody recognized the single 105-kDa protein (Figure 2A; supplemental Figure 1C). When stimulated with PAR1-AP, α-actinin was rapidly dephosphorylated. Although we have not excluded that this band was coprecipitated α-actinin with phosphoproteins, the phosphorylation profiles of immunoprecipitated α-actinin were almost the same as the faint band at 105 kDa in supplemental Figure 1B, suggesting that α-actinin itself was phosphorylated. α-Actinin was rephosphorylated at 20 minutes after PAR1-AP stimulation, whereas PAR4-AP induced sustained dephosphorylation of α-actinin. In addition to these agonists, we also examined adenosine diphosphate (ADP) and U46619-induced αIIbβ3 activation (supplemental Figure 2). ADP and U46619 induced transient and sustained αIIbβ3 activation, respectively. Again, α-actinin dissociation and de-phosphorylation induced by ADP and U46619 were transient and sustained, respectively. Thus, the kinetics of α-actinin phosphorylation seemed to synchronize with its interaction with αIIbβ3 (Figures 1E,2A).

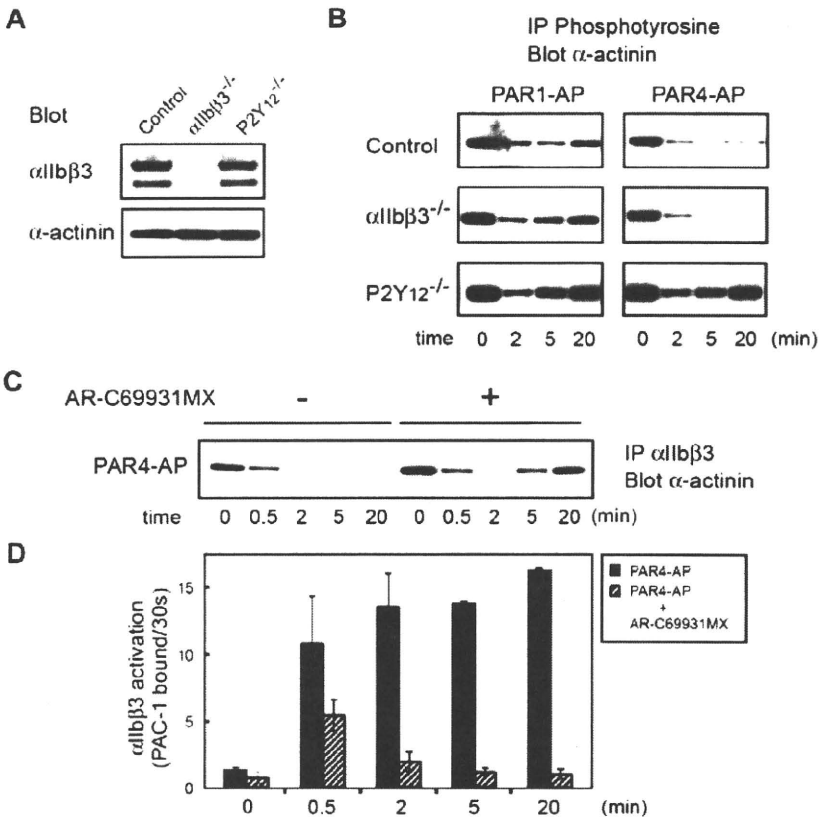

Figure 3. Changes in α-actinin phosphorylation and its interaction with αIIbβ3 in platelets from patients with Glanzmann thrombasthenia or $P2Y_{12}$ deficiency. (A) Platelet lysates from patients with Glanzmann thrombasthenia or patients with $P2Y_{12}$ deficiency were subjected to SDS–polyacrylamide gel electrophoresis and immunoblotted with anti-αIIbβ3 antibody or anti–α-actinin antibody. (B) Washed platelets were stimulated with PAR1-AP (25 μM) or PAR4-AP (150 μM) for the time indicated. Tyrosine-phosphorylated proteins were immunoprecipitated then immunoblotted with anti–α-actinin antibody. (C) Washed normal platelets were stimulated with PAR4-AP (150 μM) for the time indicated after incubation with AR-C69931MX (1 μM) for 2 minutes. αIIbβ3 was immunoprecipitated then immunoblotted with anti–α-actinin antibody. (D) Washed normal platelets were stimulated with PAR4-AP (150 μM) for the time indicated after incubation with AR-C69931MX (1 μM) for 2 minutes. FITC–PAC-1 was added to the activated platelets after stimulation and incubated for 30 seconds to obtain the PAC-1 binding velocity at the time indicated. Error bars represent SEMs of 3 experiments.

It has been shown that the PTP SHP-1 regulates the dephosphorylation of α-actinin.[23] To examine whether dephosphorylation of α-actinin regulates the dissociation of α-actinin from αIIbβ3 and integrin activation, we examined the effects of PTPI-1, a specific inhibitor of SHP-1[31] and PTP1B. Figure 2B shows that PTPI-1 inhibited the dephosphorylation of α-actinin. In addition, PTPI-1 markedly inhibited the activation of αIIbβ3 as well as the dissociation of α-actinin (Figure 2C). These results suggest that tyrosine phosphorylation of α-actinin regulates the interaction between α-actinin and αIIbβ3.

Interaction between α-actinin and integrin in platelets from a patient with Glanzmann thrombasthenia or $P2Y_{12}$ deficiency

To examine further the role of α-actinin in inside-out signaling, we analyzed platelets from a patient with Glanzmann thrombasthenia or $P2Y_{12}$-ADP receptor deficiency.[24] Figure 3A shows the expression profiles of αIIbβ3 and α-actinin in both patients. In Glanzmann thrombasthenia platelets, the phosphotyrosine profile of α-actinin was almost the same as that of control platelets under both PAR1-AP and PAR4-AP stimulation, confirming that αIIbβ3 outside-in signaling does not mediate these changes. In sharp contrast, PAR4-AP stimulation failed to induce the sustained dephosphorylation of α-actinin in $P2Y_{12}$-deficient platelets. Similarly, compared with control platelets, dephosphorylation of α-actinin induced by PAR1-AP was also disrupted at earlier time points in $P2Y_{12}$-deficient platelets (Figure 3B). This early disruption of the dephosphorylation of α-actinin is consistent with our previous finding that $P2Y_{12}$-mediated signaling is essential for sustained αIIbβ3 activation.[29] Indeed, the blockade of $P2Y_{12}$ with AR-C69931MX impaired the PAR4-AP–induced sustained αIIbβ3 activation, leading to the reassociation of α-actinin with αIIbβ3 (Figure 3C-D).

We have previously reported that the sustained αIIbβ3 activation induced by thrombin could be disrupted by inhibiting $P2Y_{12}$-mediated signaling even after thrombin stimulation.[29] Washed platelets were stimulated with thrombin at 0.2 U/mL. Two minutes later, we added AR-C69931MX (1 μM) to the thrombin-stimulated platelets. We confirmed that AR-C69931MX still disrupted the sustained αIIbβ3 activation even under these conditions (Figure 4A). Interestingly, the sustained dephosphorylation and the dissociation of α-actinin from αIIbβ3 were disrupted by adding AR-C69931MX (Figure 4B-C). The blockade of $P2Y_{12}$ was confirmed by the VASP phosphorylation state.[32] These results suggest that the interaction between α-actinin and αIIbβ3 is, at least in part, regulated by $P2Y_{12}$-mediated signaling but not by αIIbβ3 outside-in signaling.

α-Actinin modulates agonist-induced αIIbβ3 activation in CMK cells

Finally, we used direct genetic manipulation to examine the effect of α-actinin on αIIbβ3 activation in human megakaryoblastic cell line CMK cells. Because the tyrosine residue at position 12 was reported as the main site of tyrosine phosphorylation in α-actinin,[23] we overexpressed wild-type α-actinin and Y12F α-actinin in CMK cells. As shown in Figure 5A, the expression of α-actinin was increased to 130%-170% of endogenous levels without affecting αIIbβ3 expression. Next, we examined the interaction between α-actinin and αIIbβ3 in CMK cells. Like platelets and primary megakaryocytes,[4] CMK cells can activate αIIbβ3 by the stimulation of physiologic agonists such as PAR1-AP.[27,30] Similar to platelets, α-actinin was associated with αIIbβ3 in unstimulated CMK cells. When stimulated with PAR1-AP, α-actinin dissociated from αIIbβ3. Overexpression of wild-type α-actinin, but not the

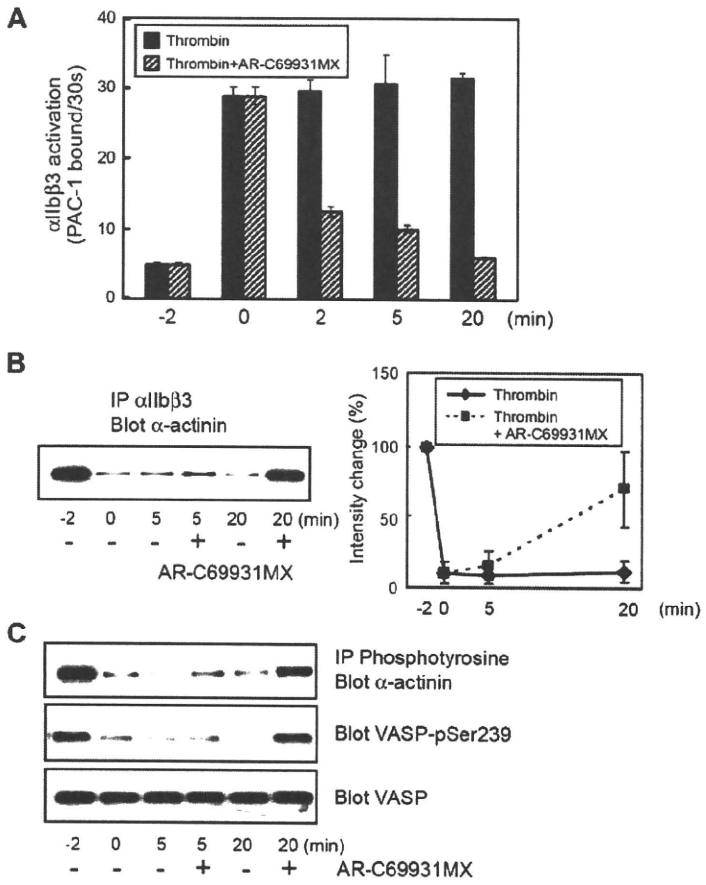

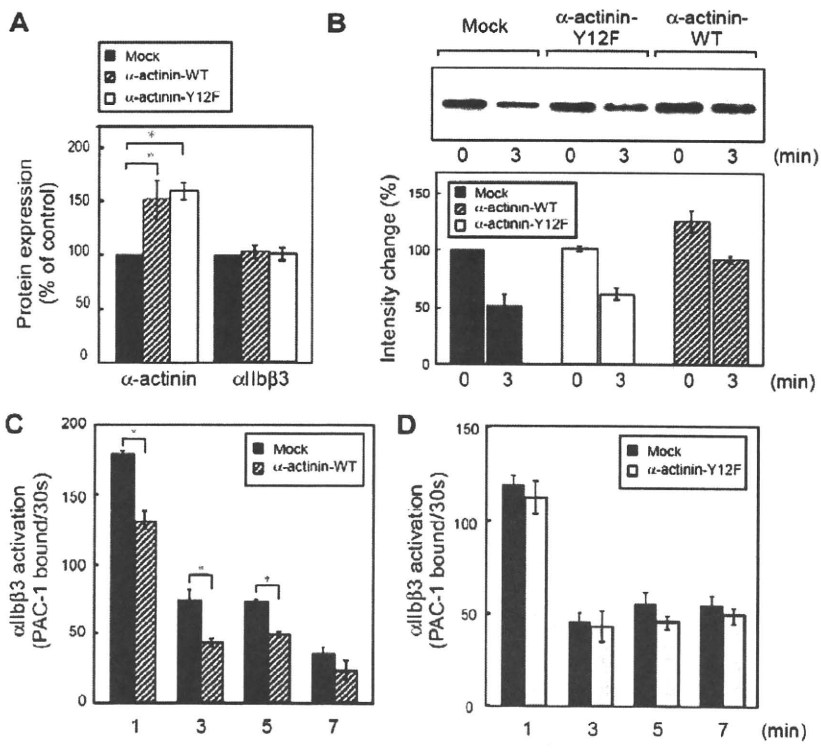

Figure 4. Effects of the blockade of $P2Y_{12}$ on α-actinin and αIIbβ3. Washed human platelets were incubated with thrombin (0.2 U/mL). The $P2Y_{12}$ antagonist, AR-C69931MX (1 μM), was added after 2 minutes of thrombin stimulation. (A) FITC–PAC-1 was added to the activated platelets after stimulation and incubated for 30 seconds to obtain the PAC-1 binding velocity at the time indicated. (B) αIIbβ3 was immunoprecipitated then immunoblotted with anti–α-actinin antibody. (C) Tyrosine-phosphorylated proteins were immunoprecipitated then immunoblotted with anti–α-actinin antibody. Preimmunoprecipitated lysates were also subjected to SDS–polyacrylamide gel electrophoresis and immunoblotted with anti–phospho-VASP (Ser239) antibody or anti-VASP antibody. Error bars represent SEMs of 3 experiments.

Figure 5. Effects of α-actinin on αIIbβ3 inside-out signaling in CMK cells. Human megakaryoblastic CMK cells were transiently transfected with plasmids encoding for α-actinin and Tac subunit of the human interleukin-2 receptor. Protein expression and integrin activation were assessed 20 hours after transfection. (A) Intracellular α-actinin and surface αIIbβ3 were determined by flow cytometry. Bar charts represent specific antibody binding to highly transfected cells (CD25-allophycocyanin fluorescence > 50) normalized to mock plasmid (pcDNA3.1)–transfected cells. Transfected CMK cells were incubated with PAR1-AP (50 μM) for the time indicated. αIIbβ3 was immunoprecipitated then immunoblotted with anti–α-actinin antibody(B). Bar charts represent PAC-1 binding to wild-type α-actinin (C) or mutant α-actinin (D) transfected cells. Error bars represent SEMs of 3 experiments. $^*P < .05$.

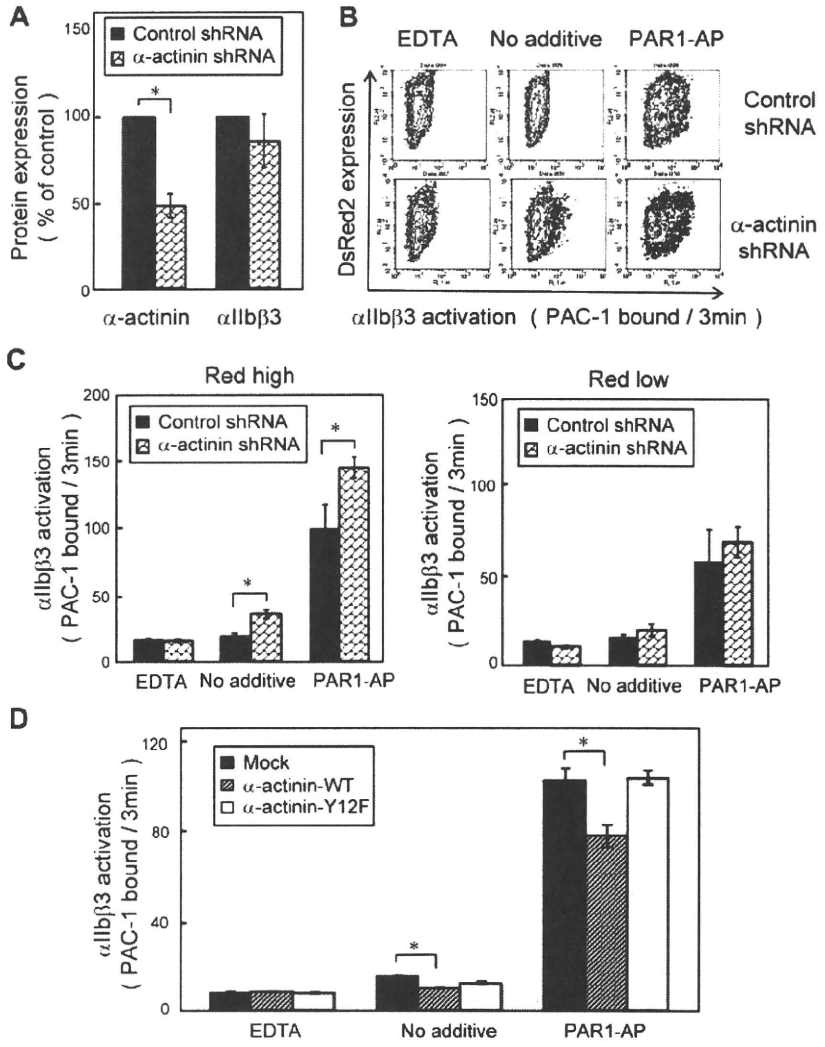

Figure 6. Knockdown of α-actinin augmented PAR1-AP–induced PAC-1 binding in CMK. Lentiviral particles encoding a shRNA for α-actinin or a control shRNA were transduced to CMK cells. (A) Intracellular α-actinin and surface αIIbβ3 were determined by flow cytometry. (B) CMK cells were stimulated with PAR1-AP (50μM) under nonstirring conditions with FITC–PAC-1 for 3 minutes. In contour plots, PAC-1 binding is shown on the x-axis, and transduction of the lentiviral particles is estimated by DsRed2 expression on the y-axis. (C) Bar charts represent PAC-1 binding to highly transduced cells (DsRed2 fluorescence > 250) and to less transduced cells (DsRed2 fluorescence < 50). (D) α-Actinin shRNA–transduced CMK cells were transiently transfected with plasmid encoding for wild-type or mutant α-actinin. Cells were stimulated with PAR1-AP (50μM) under nonstirring conditions with FITC–PAC-1 for 3 minutes. Error bars represent SEMs of 3 experiments in PAR1-AP and EDTA and of 8 experiments in no additive condition. $^*P < .05$.

mutant Y12F α-actinin, increased the basal association between α-actinin and αIIbβ3 (Figure 5B).

We then performed PAC-1 binding velocity analysis on the gated subset of live, transfected, and CD42b$^+$ CMK cells stimulated with PAR1-AP, as described in the experimental procedures. CMK cells bound little PAC-1 in the absence of agonists. When stimulated with PAR1-AP, most mock-transfected cells bound PAC-1 (supplemental Figure 3A). Overexpression of wild-type α-actinin decreased PAC-1 binding velocity (Figure 5C) as well as the amounts of PAC-1 binding in the conventional PAC-1 binding assay (supplemental Figure 3C). The α-actinin expression has a concentration-dependent effect. High expression of α-actinin suppressed PAC-1 binding induced by PAR1-AP, but low expression of α-actinin did not (supplemental Figure 3B). In contrast, overexpression of the mutant Y12F α-actinin did not decrease PAC-1 binding velocity (Figure 5D). To examine further the effects of α-actinin, α-actinin expression was knocked down by shRNA in CMK cells. Knockdown was maximal at 10 days after infection, and shRNA induced 40%-60% reduction in the α-actinin expression (Figure 6A). Although adequate α-actinin reduction may not be obtained in CMK cells, decreased level of α-actinin augmented αIIbβ3 activation induced by PAR1-AP. Again, transduction levels (DsRed2 expression) have a concentration-dependent effect. High expression of DsRed2 augmented PAC-1 binding induced by PAR1-AP, but low expression of DsRed2 did not (Figure 6B-C). In contrast to PAR1-AP, PAR4-AP induced little PAC-1 binding velocity in CMK cells when stimulated with such high concentration as 1mM (supplemental Figure 4A). We assessed whether knockdown of α-actinin affects this PAR4-AP condition in CMK. PAC-1 binding induced by PAR4-AP was significantly augmented in the knockdown cells as well as PAR1-AP (supplemental Figure 4B). Finally wild-type α-actinin and Y12F α-actinin were overexpressed in α-actinin shRNA-transduced CMK cells. Wild-type α-actinin, but not the mutant Y12F α-actinin, normalized the augmented αIIbβ3 activation induced by PAR1-AP in CMK cells (Figure 6D). These results suggest that the binding of α-actinin might be involved in αIIbβ3 activation.

Discussion

Here, we focused on α-actinin as a member of the IAC and assessed its potential role in integrin-reversible activation. Resting αIIbβ3 was already associated with α-actinin, and inside-out

signaling by PARs induced a dissociation of α-actinin from αIIbβ3. This dissociation was regulated by dephosphorylation of α-actinin and associated with reversible αIIbβ3 activation, as evidenced by the stimulation of PAR1-AP and PAR4-AP. Overexpression of wild-type α-actinin, but not a mutant with a tyrosine-phosphorylation defect (Y12F), inhibited αIIbβ3 activation in a megakaryocytic cell line, CMK, in which αIIbβ3 is activated by PAR1-AP. Knockdown of α-actinin augmented PAR-AP–induced PAC-1 binding in CMK. Thus, our observations suggest that α-actinin may play a role in keeping αIIbβ3 in a low-affinity state.

Thrombin activates human platelets through proteolytic activation of 2 protease-activated receptors, PAR1 and PAR4.[33] PAR1 is a high-affinity receptor for platelet activation at low concentrations of thrombin, whereas PAR4 is a low-affinity receptor that mediates thrombin signaling at high concentrations. Consistent with previous reports,[34,35] we showed distinct kinetics of signaling from these PARs by evaluation of intracellular calcium mobilization and P-selectin translocation. PAR1 triggered a rapid and transient increase in intracellular calcium, whereas PAR4 triggered a slower but more prolonged response. Accordingly, we used PAR1-AP and PAR4-AP to examine the role of α-actinin in integrin activation. To assess the activation state of αIIbβ3 more precisely, we performed initial velocity analysis at a specific time point. The kinetic approach with the use of flow cytometry has been proposed for assessing the dynamics of αIIbβ3 activation,[36] and we have modified it as the initial velocity analysis for assessing reversible αIIbβ3 activation. On-rate of PAC-1 binding reflects the number of activated receptors, and the initial velocity analysis showed that PAR1 stimulation induced only transient activation. In addition, only 25% of αIIbβ3 was kept activated at 20 minutes after stimulation compared with the amount of activated αIIbβ3 at 2 minutes after stimulation.

In contrast, PAR4 induced long-lasting αIIbβ3 activation, and the amount of activated αIIbβ3 was almost the same at 2 minutes and 20 minutes after stimulation. The association/dissociation behavior of α-actinin with αIIbβ3 is apparently related to the distinct αIIbβ3 activation kinetics induced by PAR1-AP, PAR4-AP, ADP, and U46619.

We have shown that continuous interaction between released endogenous ADP and $P2Y_{12}$ is critical for sustained αIIbβ3 activation induced by thrombin.[29] In this context, the sustained αIIbβ3 activation induced by PAR4-AP was markedly impaired in $P2Y_{12}$-deficient platelets. In addition, the dissociation and dephosphorylation of α-actinin induced by PAR4-AP as well as by PAR1-AP was markedly impaired. Moreover, after αIIbβ3 activation was completed by thrombin stimulation, the addition of AR-C69931MX disrupted the dissociation and dephosphorylation of α-actinin as well as the sustained αIIbβ3 activation. PTPI-1, an inhibitor of SHP-1, inhibited the dissociation as well as the dephosphorylation of α-actinin induced by PAR1-AP. These data suggest a close association between the dissociation and dephosphorylation of α-actinin and regulation of these changes, at least in part, by $P2Y_{12}$-mediated signaling.

Cellular control of integrin activation requires transmission of a signal from the cytoplasmic tails to the extracellular domains. One may argue that the activation state of αIIbβ3 is an intrinsic state of the integrin itself and not a property of platelets per se.[37] However, this concept is based on the property of exogenous αIIbβ3 expressed on Chinese hamster ovary cells which is not activated by several platelet agonists. In this study, we have demonstrated that endogenous αIIbβ3 expressed on CMK cells can be activated by PAR-APs. Recent studies have identified some intracellular adapters, enzymes, and substrates necessary for αIIbβ3 activation and the tails function as regulatory scaffolds.[38] Among cytoplasmic proteins associated with β3 tail, talin[4,8] and kindlins[9] are now well established as being essential for integrin activation. Recently, it has been shown that talin binding is sufficient to activate integrin αIIbβ3[39] and that a talin membrane contact would be required for integrin activation.[39,40] In this context, α-actinin may modulate the accessibility of talin to the β3 tail or to plasma membrane because putative α-actinin binding sites have been reported within the membrane proximal region of the β3 cytoplasmic tail.[15,41] In platelets α-actinin was no longer associated with αIIbβ3 after PAR-AP stimulation. This may imply that α-actinin knockdown would not further enhance the extent of integrin activation. However, α-actinin knockdown significantly augmented PAC-1 binding induced by 1mM PAR4-AP as well as 50μM PAR1-AP in CMK. Unlike platelets, CMK needed a higher concentration of agonists to get enough levels of activated αIIbβ3. Even under those conditions, the levels of activated αIIbβ3 were less, and the sustained time of activation was shorter than platelets. From these observations, we assume that αIIbβ3 in CMK cells under our experimental conditions may not be fully activated. It is possible that this is the reason why α-actinin knockdown further enhances integrin activation in CMK cells. Thus, the α-actinin binding to the β3 tail may keep αIIbβ3 in a low-affinity state, and it is possible that the dissociation of α-actinin from the β3 tail may lead to the easy accessibility of talin to the β3 tail by inside-out signaling. Like β3 integrin, β2 integrins can change affinity on a subsecond time scale.[1] Recent studies have shown that intermediate-affinity lymphocyte function-associated antigen-1 bound to α-actinin, whereas high-affinity lymphocyte function antigen-1 bound to talin.[17,18] These data show that α-actinin and talin regulate integrin activation differently.

α-Actinin colocalizes with actin and stabilizes the actin filament web in nonmuscle cells.[13] It has been suggested that most α-actinin forms a bridge between the actin filaments and that there is some α-actinin associated with integrin at the end of actin filaments.[14] Indeed, we have confirmed that most α-actinin was not associated with αIIbβ3, as evidenced by the presence of large amounts of α-actinin in the supernatant even in immunoprecipitates of αIIbβ3 from resting platelets (data not shown). In the fibroblast, the phosphorylation of α-actinin reduces its affinity for actin and prevents its localization to focal adhesion plaques.[42] Another report showed that the phosphorylation of α-actinin might serve to modulate the coupling/uncoupling of integrins to the cytoskeleton in platelets.[23] Outside-in signaling involving interaction of αIIbβ3 with its immobilized ligand fibrinogen triggers tyrosine phosphorylation and cytoskeletal reorganization in platelets.[20] Pathologic shear forces, such as those encountered in stenotic midsized coronary and cerebral arteries, directly affect ligand-dependent αIIbβ3 outside-in signaling, and a recent study showed that pathologic shear stress induced dissociation of α-actinin from the β3 tail, which is αIIbβ3 dependent.[43] Our observations described here are clearly different phenomena from those induced by outside-in signaling; an αIIbβ3-specific antagonist, FK633, did not inhibit the dissociation, and dephosphorylation was induced even in thrombasthenic platelets. Thus, both inside-out signaling and outside-in signaling regulate the dissociation of α-actinin from αIIbβ3.

Integrin function is a complex process regulated by the balance of positive and negative regulatory proteins. Several factors have been identified as positive and negative regulators of αIIbβ3.[44,45] Platelet agonists, such as thrombin and ADP, induce αIIbβ3 activation, whereas various vasodilators released from the endothelial cells keep αIIbβ3 inactive in circulating blood. In addition to platelet agonists and vasodilators, the balance of positive and negative

regulatory proteins in IAC may regulate αIIbβ3 activation. Our observations described here suggest that α-actinin may act as a negative regulator in resting platelets. Although further work is needed to determine each specific role of α-actinin in platelets, the α-actinin–integrin interaction might be added to the discussion of new potential targets for atherothrombotic disease therapies.

Acknowledgments

This work was supported by Grant-in Aid for Scientific Research from the Ministry of Education, Culture, Sports, Science and Technology in Japan, from the Ministry of Health, Labor and Welfare in Japan; and "Academic Frontier" Project in Japan.

Authorship

Contribution: S.T. designed and performed experiments, analyzed data, and wrote the paper; T.N., T.K., and K.K. helped perform parts of the experiments; H.K. and S.H. provided feedback and experimental advice; and Y.K. and Y.T. supervised the project and reviewed the paper.

Conflict-of-interest disclosure: The authors declare no competing financial interests.

Correspondence: Seiji Tadokoro, Department of Hematology and Oncology, Osaka University Graduate School of Medicine C9, 2-2 Yamada-oka, Suita Osaka 565-0871, Japan; e-mail: tadokoro@hp-blood.med.osaka-u.ac.jp.

References

1. Hynes RO. Integrins: bidirectional, allosteric signaling machines. *Cell.* 2002;110(6):673-687.
2. Shattil SJ, Newman PJ. Integrins: dynamic scaffolds for adhesion and signaling in platelets. *Blood.* 2004;104(6):1606-1615.
3. O'Toole TE, Katagiri Y, Faull RJ, et al. Integrin cytoplasmic domains mediate inside-out signal transduction. *J Cell Biol.* 1994;124(6):1047-1059.
4. Tadokoro S, Shattil SJ, Eto K, et al. Talin binding to integrin beta tails: a final common step in integrin activation. *Science.* 2003;302(5642):103-106.
5. Moser M, Legate KR, Zent R, Fässler R. The tail of integrins, talin, and kindlins. *Science.* 2009; 324(5929):895-899.
6. Wegener KL, Partridge AW, Han J, et al. Structural basis of integrin activation by talin. *Cell.* 2007;128(1):171-182.
7. Petrich BG, Marchese P, Ruggeri ZM, et al. Talin is required for integrin-mediated platelet function in hemostasis and thrombosis. *J Exp Med.* 2007; 204(13):3103-3111.
8. Nieswandt B, Moser M, Pleines I, et al. Loss of talin1 in platelets abrogates integrin activation, platelet aggregation, and thrombus formation in vitro and in vivo. *J Exp Med.* 2007;204(13):3113-3118.
9. Moser M, Nieswandt B, Ussar S, Pozgajova M, Fässler R. Kindlin-3 is essential for integrin activation and platelet aggregation. *Nat Med.* 2008; 14(3):325-330.
10. Ma YQ, Qin J, Wu C, Plow EF. Kindlin-2 (Mig-2): a co-activator of beta3 integrins. *J Cell Biol.* 2008; 181(3):439-446.
11. Harburger DS, Bouaouina M, Calderwood DA. Kindlin-1 and -2 directly bind the C-terminal region of beta integrin cytoplasmic tails and exert integrin-specific activation effects. *J Biol Chem.* 2009;284(17):11485-11497.
12. Kiema T, Lad Y, Jiang P, et al. The molecular basis of filamin binding to integrins and competition with talin. *Mol Cell.* 2006;21(3):337-347.
13. Otey CA, Carpen O. alpha-Actinin revisited: a fresh look at an old player. *Cell Motil Cytoskeleton.* 2004;58(2):104-111.
14. Sjöblom B, Salmazo A, Djinović-Carugo K. alpha-Actinin structure and regulation. *Cell Mol Life Sci.* 2008;65(17):2688-2701.
15. Otey CA, Pavalko FM, Burridge K. An interaction between alpha-actinin and the beta1 integrin subunit in vitro. *J Cell Biol.* 1990;111(2):721-729.
16. Pavalko FM, LaRoche SM. Activation of human neutrophils induces an interaction between the integrin beta2-subunit (CD18) and the actin binding protein alpha-actinin. *J Immunol.* 1993;151(7):3795-3807.
17. Smith A, Carrasco YR, Stanley P, Kieffer N, Batista FD, Hogg N. A talin-dependent LFA-1 focal zone is formed by rapidly migrating T lymphocytes. *J Cell Biol.* 2005;170(1):141-151.
18. Stanley P, Smith A, McDowall A, Nicol A, Zicha D, Hogg N. Intermediate-affinity LFA-1 binds alpha-actinin-1 to control migration at the leading edge of the T cell. *EMBO J.* 2008;27(1):62-75.
19. Shattil SJ, Ginsberg MH, Brugge JS. Adhesive signaling in platelets. *Curr Opin Cell Biol.* 1994; 6(5):695-704.
20. Haimovich B, Lipfert L, Brugge JS, Shattil SJ. Tyrosine phosphorylation and cytoskeletal reorganization in platelets are triggered by interaction of integrin receptors with their immobilized ligands. *J Biol Chem.* 1993;268(21):15868-15877.
21. Izaguirre G, Aguirre L, Ji P, Aneskievich B, Haimovich B. Tyrosine phosphorylation of alpha-actinin in activated platelets. *J Biol Chem.* 1999;274(52):37012-37020.
22. Izaguirre G, Aguirre L, Hu YP, et al. The cytoskeletal/non-muscle isoform of alpha-actinin is phosphorylated on its actin-binding domain by the focal adhesion kinase. *J Biol Chem.* 2001;276(31):28676-28685.
23. Lin SY, Raval S, Zhang Z, et al. The protein-tyrosine phosphatase SHP-1 regulates the phosphorylation of alpha-actinin. *J Biol Chem.* 2004; 279(24):25755-25764.
24. Shiraga M, Miyata S, Kato H, et al. Impaired platelet function in a patient with P2Y12 deficiency caused by a mutation in the translation initiation codon. *J Thromb Haemost.* 2005;3(10):2315-2323.
25. Tokuhira M, Handa M, Kamata T, et al. A novel regulatory epitope defined by a murine monoclonal antibody to the platelet GPIIb-IIIa complex (alphaIIbbeta3 integrin). *Thromb Haemost.* 1996; 76(6):1038-1046.
26. Honda S, Tomiyama Y, Aoki T, et al. Association between ligand-induced conformational changes of integrin alphaIIbbeta3 and alphaIIbbeta3-mediated intracellular Ca^{2+} signaling. *Blood.* 1998;92(10): 3675-3683.
27. Kashiwagi H, Shiraga M, Honda S, et al. Activation of integrin alphaIIbbeta3 in the glycoprotein Ib-high population of a megakaryocytic cell line, CMK, by inside-out signaling. *J Thromb Haemost.* 2004;2(1):177-186.
28. LaFlamme SE, Akiyama SK, Yamada KM. Regulation of fibronectin receptor distribution. *J Cell Biol.* 1992;117(2):437-447.
29. Kamae T, Shiraga M, Kashiwagi H, et al. Critical role of ADP interaction with P2Y12 receptor in the maintenance of alphaIIbbeta3 activation: association with Rap1B activation. *J Thromb Haemost.* 2006;4(6):1379-1387.
30. Shiraga M, Kamae T, Akiyama M, et al. P2Y12-independent transient activation and P2Y12-dependent prolonged activation of platelet integrin alphaIIbbeta3 [abstract]. *Blood.* 2006;108(11):435a. Abstract 1509.
31. Arabaci G, Guo XC, Beebe KD, Coggeshall KM, Pei D. alpha-Haloacetophenone derivatives as photoreversible covalent inhibitors of protein tyrosine phosphatases. *J Am Chem Soc.* 1999; 121(21):5085-5086.
32. Aleil B, Ravanat C, Cazenave JP, Rochoux G, Heitz A, Gachet C. Flow cytometric analysis of intraplatelet VASP phosphorylation for the detection of clopidogrel resistance in patients with ischemic cardiovascular diseases. *J Thromb Haemost.* 2005;3(1):85-92.
33. Kahn ML, Zheng YW, Huang W, et al. A dual thrombin receptor system for platelet activation. *Nature.* 1998;394(6694):690-694.
34. Covic L, Gresser AL, Kuliopulos A. Biphasic kinetics of activation and signaling for PAR1 and PAR4 thrombin receptors in platelets. *Biochemistry.* 2000;39(18):5458-5467.
35. Shapiro MJ, Weiss EJ, Faruqi TR, Coughlin SR. Protease activated receptor 1 and 4 are shut off with distinct kinetics after activation by thrombin. *J Biol Chem.* 2000;275(33):25216-25221.
36. Frojmovic M, Wong T, van de Ven T. Dynamic measurements of the platelet membrane glycoprotein IIb-IIIa receptor for fibrinogen by flow cytometry, I: methodology, theory and results for two distinct activators. *Biophys J.* 1991;59(4):815-827.
37. O'Toole TE, Loftus JC, Du XP, et al. Affinity modulation of the alphaIIbbeta3 integrin (platelet GPIIb-IIIa) is an intrinsic property of the receptor. *Cell Regul.* 1990;1(12):883-893.
38. Legate KR, Fässler R. Mechanisms that regulate adaptor binding to beta-integrin cytoplasmic tails. *J Cell Sci.* 2009;122(Pt 2):187-198.
39. Ye F, Hu G, Taylor D, et al. Recreation of the terminal events in physiological integrin activation. *J Cell Biol.* 2010;188(1):157-173.
40. Lau TL, Kim C, Ginsberg MH, Ulmer TS. The structure of the integrin alphaIIbbeta3 transmembrane complex explains integrin transmembrane signalling. *EMBO J.* 2009;28(9):1351-1361.
41. Lyman S, Gilmore A, Burridge K, Gidwitz S, White GCII. Integrin-mediated activation of focal adhesion kinase is independent of focal adhesion formation or integrin activation. Studies with activated and inhibitory beta3 cytoplasmic domain mutants. *J Biol Chem.* 1997;272(36):22538-22547.
42. von Wichert G, Haimovich B, Feng GS, Sheetz MP. Force-dependent integrin-cytoskeleton linkage formation requires downregulation of focal complex dynamics by Shp2. *EMBO J.* 2003;22(19):5023-5035.
43. Feng S, Lu X, Reséndiz JC, Kroll MH. Pathological shear stress directly regulates platelet alphaIIbbeta3 signaling. *Am J Physiol Cell Physiol.* 2006;291(6):C1346-C1354.
44. Tomiyama Y, Shiraga M, Kashiwagi H. Positive and negative regulation of integrin function. In: Tanaka K, Davie EW, eds. *Recent Advances in Thrombosis and Hemostasis 2008.* New York, NY: Springer;2008:243-252.
45. Brass LF, Zhu L, Stalker TJ. Minding the gaps to promote thrombus growth and stability. *J Clin Invest.* 2005;115(12):3385-3392.

Int J Hematol (2011) 93:106–111
DOI 10.1007/s12185-010-0731-5

CASE REPORT

Molecular analysis of a patient with type I Glanzmann thrombasthenia and clinical impact of the presence of anti-αIIbβ3 alloantibodies

Hirokazu Kashiwagi · Kazunobu Kiyomizu · Tsuyoshi Kamae · Tsuyoshi Nakazawa · Seiji Tadokoro · Shuji Takiguchi · Yuichiro Doki · Yuzuru Kanakura · Yoshiaki Tomiyama

Received: 28 October 2010 / Revised: 12 November 2010 / Accepted: 12 November 2010 / Published online: 8 December 2010

Abstract The occurrence of transfusion-related alloimmunization against αIIbβ3 is a major concern in patients with Glanzmann thrombasthenia (GT). However, few data are available about molecular defects of GT patients with anti-αIIbβ3 alloantibodies as well as clinical impact of these antibodies on platelet transfusion. Here, we report a case of type I GT with anti-HLA and anti-αIIbβ3 alloantibodies, who underwent laparoscopic total gastrectomy due to gastric cancer. We found a novel β3 nonsense mutation, 892C > T (Arg272X), and the patient was homozygous for the mutation. Laparoscopic gastrectomy was successfully performed with continuous infusion of HLA-matched platelet concentrates and bolus injection of recombinant factor VIIa at 2 h intervals. Total bleeding was 370 mL and no red-cell transfusion was necessary. Flow cytometric analysis employing anti-αIIbβ3 monoclonal antibody revealed that the transfused platelet count was maintained around 20–30 × 10^9/L during the operation and 10 × 10^9/L on the following day. Flow cytometric analysis also showed that transfused platelets retained normal reactivity to ADP stimulation. These results indicate that flow cytometry is useful to assess survival and function of transfused platelets in GT patients with anti-αIIbβ3 antibodies.

Keywords Glanzmann thrombasthenia · Anti-αIIbβ3 alloantibody · Mutation · Platelet transfusion · Recombinant factor VIIa

H. Kashiwagi · K. Kiyomizu · T. Kamae · T. Nakazawa · S. Tadokoro · Y. Kanakura · Y. Tomiyama
Department of Hematology and Oncology, Graduate School of Medicine, Osaka University, Suita, Osaka, Japan

S. Takiguchi · Y. Doki
Department of Gastroenterological Surgery, Graduate School of Medicine, Osaka University, Suita, Osaka, Japan

Y. Tomiyama (✉)
Department of Blood Transfusion, Osaka University Hospital, 2-15 Yamada-oka, Suita, Osaka 565-0871, Japan
e-mail: yoshi@hp-blood.med.osaka-u.ac.jp

1 Introduction

Glanzmann thrombasthenia (GT) is a rare hereditary bleeding disorder that is due to a quantitative and/or qualitative defect in integrin αIIbβ3 [glycoprotein (GP) IIb/IIIa, CD41/CD61]. GT is classified by the content of αIIbβ3: type I with <5% of normal controls, type II with 5–20%, and variant type with qualitative defect [1]. Clinical presentation includes mild to severe mucosal bleeds, traumatic or surgical hemorrhage, and occasional life-threatening bleeding episodes. Although treatment such as local measures and/or antifibrinolytics agents may be beneficial for mild bleeding, platelet transfusion is often necessary for severe bleeding, delivery and surgery. However, repeated transfusions may induce alloantibodies against HLA and/or αIIbβ3, leading to refractoriness to platelet transfusion. Moreover, it may be possible that anti-αIIbβ3 antibodies functionally block the binding of physiological ligands to αIIbβ3 on transfused platelets [2]. Treatment of GT patients with alloantibodies against αIIbβ3 are challenging. Removal of antibodies by plasma pheresis or immunoadsorption may be effective, although the procedure may present difficulties [3, 4]. In such cases, recombinant factor VIIa (rFVIIa) could represent an alternative. Tengborn and Petruson [5] reported the first successful case of rFVIIa treatment for epistaxes of a GT

patient, and Poon et al. [6] confirmed the effectiveness of rFVIIa to GT patients with international survey.

Despite clinical significance of anti-αIIbβ3 alloantibodies, little is known about genetic predisposing factors and the impact of anti-αIIbβ3 alloantibodies on the survival and function of transfused platelets in GT patients. We experienced a type I GT patient with anti-HLA and anti-αIIbβ3 antibodies suffering from gastric cancer, and laparoscopic total gastrectomy was successfully performed with HLA-matched platelet transfusion and bolus infusion of rFVIIa. In this study, we revealed a novel β3 mutation which could be responsible for the patient's phenotype and compared literally reported molecular defects of GT patients with anti-αIIbβ3 alloantibodies. Moreover, we assessed the survival and function of transfused normal platelets by monitoring of CD42b (GPIb) and αIIbβ3 expression employing flow cytometry.

2 Case report

A 59-year-old Japanese man was suffering from a lifelong bleeding tendency and diagnosed as GT. He was a son of consanguineous parents. He received several red-cell and platelet transfusions since his age of 51 due to gastrointestinal bleeding. He again noticed tarry stools in 2008 and consulted a hospital. Platelet transfusion was effective to make bleeding time normal at that time, and gastrointestinal fiberscope and endoscopic biopsy identified poorly differentiated adenocarcinoma at lesser curvature of the stomach body. However, after 2 months neither increase in platelet counts nor improvement of bleeding time was obtained even after high-dose γ-globulin administration followed by platelet transfusion, and the planned gastrectomy was cancelled. The patient was then referred to our hospital.

Employing several anti-αIIbβ3 monoclonal antibodies (mAbs), we confirmed that expression of αIIbβ3 on the patient's platelets was <5%, compared with that of normal controls, indicating that the patient was type I GT (Fig. 1A). To reveal a molecular genetic defect in this GT patient, we analyzed the whole coding region of αIIb and β3 cDNA amplified from platelet mRNA. A novel β3 nonsense mutation, 892C > T, which would lead to a premature termination of translation at arginine-272 residue of β3, was identified. Sequencing of exon 6 of the *ITGB3* gene, which is the corresponding exon of the 892C > T mutation, showed that he was homozygous for the mutation (Fig. 1B). Examination of the patient's plasma revealed that anti-HLA antibodies were positive in standard lymphocytotoxicity assay and immunofluorescence assay (data not shown). We also found that the patient's plasma antibodies apparently reacted with αIIbβ3-

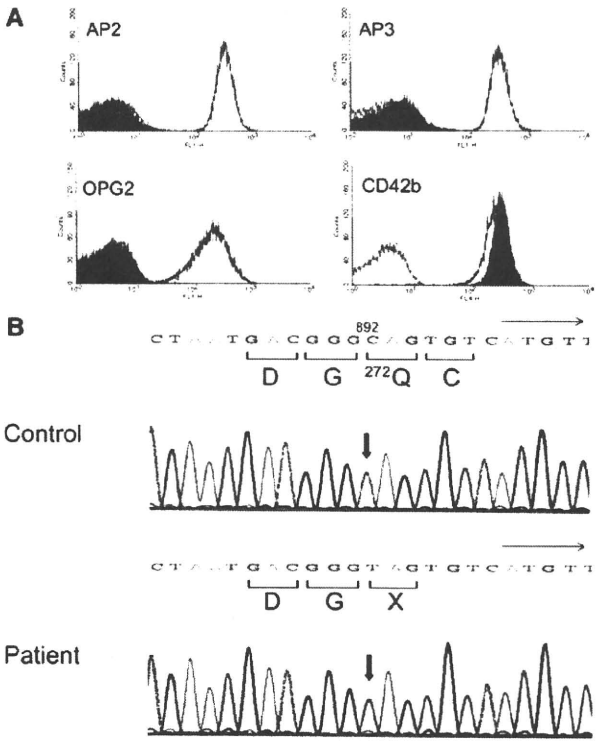

Fig. 1 Phenotype and molecular analysis of the GT patient. **A** Surface expression of glycoproteins on platelets. AP2, AP3 and OPG2 are αIIbβ3-specific, β3-specific and ligand-mimetic αIIbβ3-specific monoclonal antibodies, respectively. *Filled histograms* represent the patient's platelets. *Solid and dotted lines* represent control platelets and control IgG antibody, respectively. **B** Sequence analysis of exon 6 of the *ITGB3* gene. In the patient 892C was mutated to T, resulting in stop codon at the arginine-272 residue of β3

expressing 293 cells but not with untransfected 293T cells (Fig. 2A). Modified antigen-captured ELISA (MACE) assay [7] employing AP2, anti-αIIbβ3 mAb, as a capturing antibody clearly showed the presence of anti-αIIbβ3 antibodies as well (Fig. 2B). Therefore, we performed laparoscopic total gastrectomy under continuous infusion of two packs of HLA-matched apheresis-derived platelet concentrates containing 4.8×10^{11} and 3.5×10^{11} platelets with bolus infusion of 90 μg/kg of rFVIIa three times at 2 h intervals. The patient's platelet counts before, during, and just after the platelet transfusion were 150×10^9, 144×10^9, and 155×10^9/L, respectively, suggesting that transfused HLA-matched platelets were immediately destroyed by anti-αIIbβ3 antibodies. Then, we more precisely examined the survival of the transfused platelets employing flow cytometry. Transfused platelets were detected as CD41a (αIIbβ3) and CD42b double-positive cells, whereas autologous GT platelets were detected as CD41a-negative, CD42b-positive cells. As shown in Fig. 3A, CD41a-positive transfused platelets were 16.3 and 17.2% of total platelet counts during and just

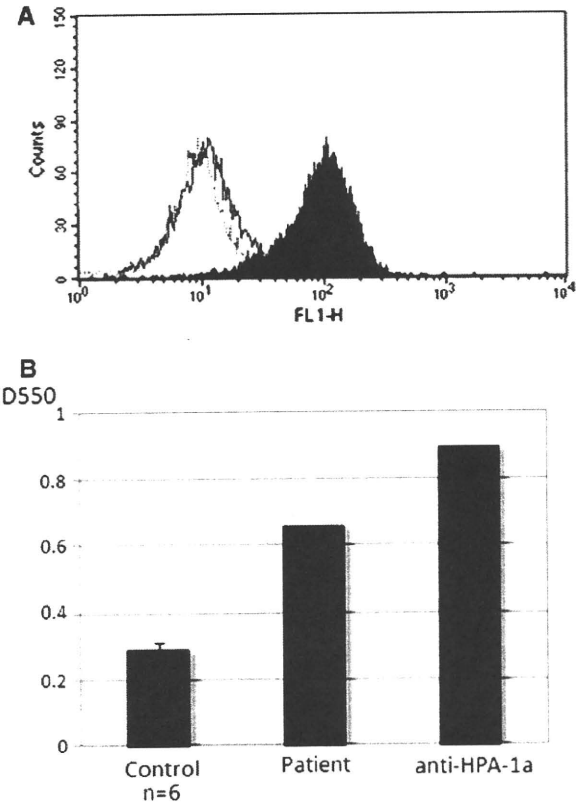

Fig. 2 Detection of anti-αIIbβ3 antibodies. **A** Plasma was incubated with αIIbβ3-stably expressed HEK293 cells. Bound IgG antibodies were detected by alexa488 anti-human IgG antibodies. *Filled and open histograms* represent the patient and normal control plasma, respectively. *Dotted line* represents the patient's plasma incubated with untransfected 293T cells. **B** Anti-αIIbβ3 antibodies were detected by MACE assay. Plasma was incubated with washed platelets obtained from blood type O subjects, and then lysed with 1% Triton X-100 buffer. Soluble fraction was added to AP2-coated microtiter well, and bound IgG was detected with biotin-conjugated anti-human IgG, followed by alkaline-phosphatase conjugated ABC kit (Vector Lab, Burlingame, CA, USA). Mean plus standard deviation of plasma obtained from 6 normal subjects is shown as negative controls. Anti-HPA-1a serum was used as positive control

after platelet transfusion, respectively. These data indicate that the numbers of the transfused platelets was estimated to 24×10^9 and 27×10^9/L (Fig. 3C). The ratio of survived CD41a-positive platelets decreased to 8.4% of total platelets on the next morning, indicating 10×10^9/L platelets were survived at that time. We also examined the function of the transfused platelets. Twenty micromolar ADP was added to the diluted whole blood samples simultaneously with FITC-PAC1, αIIbβ3 activation-dependent mAb, and PE-CD42b. The ratio of PAC1-bound platelets after ADP stimulation (13%) was comparable to that of CD41a-positive platelets (17%) during platelet transfusion, suggesting that function of the transfused platelets was not impaired by anti-αIIbβ3 alloantibodies in the patient's plasma (Fig. 3B). Although his hemoglobin concentration decreased from 14.1 to 11.0 g/dL after operation, total bleeding during the operation was 370 mL and no red-cell transfusion was necessary. Additional HLA-matched apheresis-derived platelet concentrate containing 3.0×10^{11} platelets was transfused on the following day. He was discharged after 2 weeks from the operation without any complication including bleeding.

3 Discussion

In GT patients, the occurrence of transfusion-related alloimmunization to αIIbβ3 is a major concern, as it results in the refractoriness to platelet transfusion. However, surprisingly few data are available concerning incidence, genetic factors and clinical impact of alloimmunization to αIIbβ3 in GT patients. Consistent with previous literature data that all patients with anti-αIIbβ3 alloantibodies are affected by type I GT [8, 9], our patient was type I. Although molecular basis of GT have been extensively analyzed, only seven mutations were reported in GT patients with anti-αIIbβ3 antibodies including our case [4, 9–12]. Interestingly, all patients are homozygote or compound heterozygote of premature termination mutations except one patient, who was a homozygote of β3(C575R) and produced anti-αIIbβ3 antibodies after massive platelet transfusion (Table 1). Santoro et al. [9] reported in the same literature that other two GT patients with β3(C575R) did not produce anti-αIIbβ3 antibodies after platelet transfusions. These results suggest that a mutation that causes a premature termination of translation could be a high risk for developing anti-αIIbβ3 alloantibodies. This hypothesis remains to be determined.

Effects of platelet transfusion are usually monitored simply by increase in platelet number. However, it might be difficult in case of surgery or massive bleeding, in which platelets are rapidly consumed physiologically. As reported previously [10, 13], in GT patients we can monitor survival of the infused platelets easily as αIIbβ3-positive cells by flow cytometry. Function of infused platelets might be also important, since anti-αIIbβ3 antibodies may interfere with ligand binding to αIIbβ3 [2]. Although bleeding time is usually used for monitoring platelet function, flow cytometric analysis using αIIbβ3 activation-dependent antibody, PAC-1, enabled us to assess the function of transfused platelets more easily and accurately [14]. In our case, despite that there was no increase of platelet counts after platelet transfusion, flow cytometric analysis revealed that αIIbβ3-positive platelets were maintained in $20–30 \times 10^9$/L during the surgery and 10×10^9/L on the following day (Fig. 3C). Transfused platelets showed

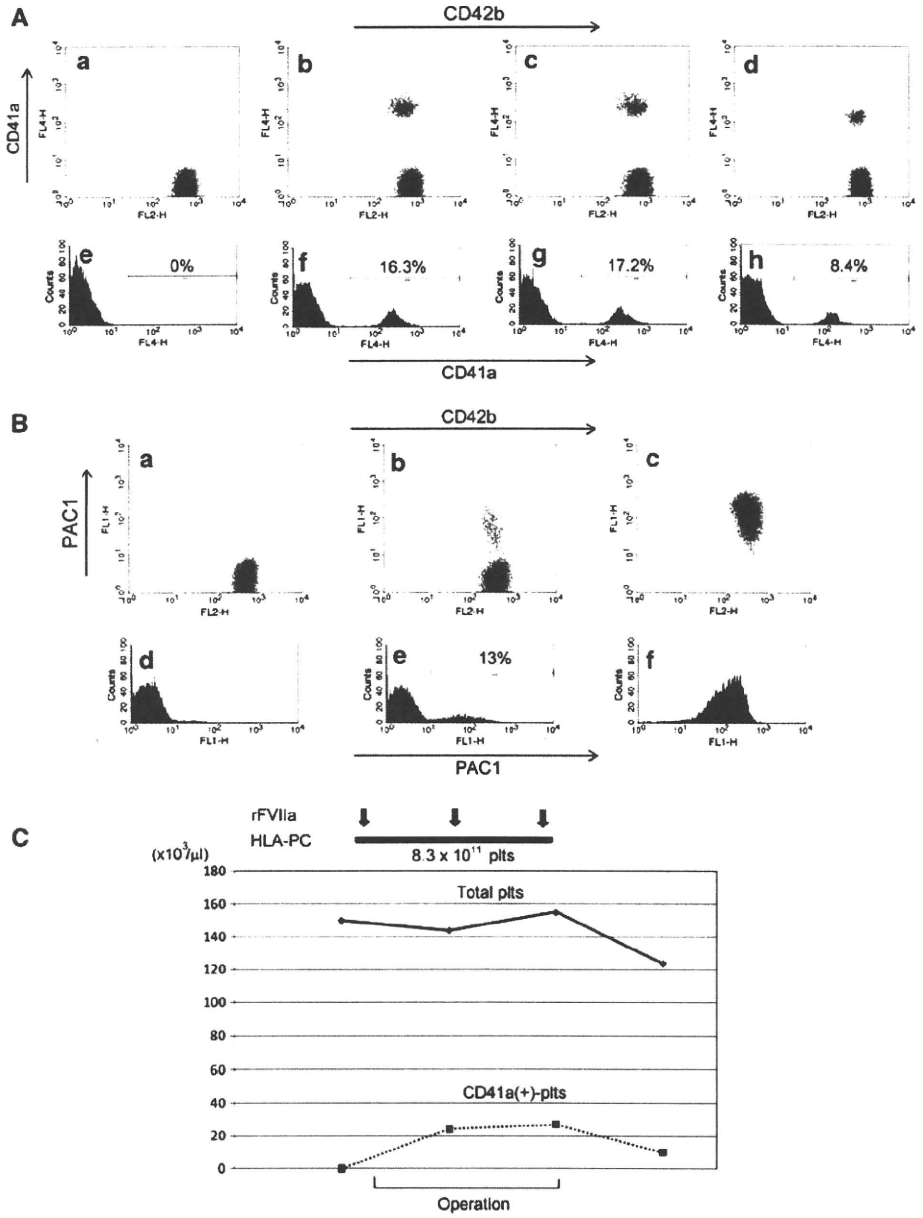

Fig. 3 Survival and function of the transfused normal platelets. **A** Detection of transfused platelets by flow cytometry. Whole blood cells diluted with Tyrodes buffer were mixed with APC-CD41a (HIP8; αIIbβ3-specific mAb) and PE-CD42b (GPIb) for 20 min. After fixed with 1% paraformaldehyde, two-color flow cytometric analysis was performed. *Upper panels* show PE-CD42b (*horizontal*)/APC-CD41a (*vertical*) dot blots. Transfused platelets were detected as CD42b(+)/CD41a(+). Lower panels show histograms of APC-CD41a and percentage of CD41a(+) platelets. *a*, *e* before operation, *b*, *f* during operation, *c*, *g* just after platelet transfusion, *d*, *h* 1-day post operation. **B** Detection of PAC1 binding after ADP stimulation. Twenty micromolar ADP was added to the diluted whole blood samples simultaneously with FITC-PAC1 and PE-CD42b. After 20 min incubation, the samples were fixed with paraformaldehyde, followed by flow cytometric analysis. *Upper panels* show PE-CD42b (*horizontal*)/FITC-PAC1 (*vertical*) dot blots and lower panels show histograms of FITC-PAC1. *a*, *d* During operation, no agonist. *b*, *e* During operation, 20 μM ADP (+). *c*, *f* Normal control, ADP (+). **C** Transition of total platelets counts and number of calculated CD41a-positive platelets. HLA-matched platelet concentrates containing 8.3×10^{11} platelets were transfused continuously during operation. Bolus infusion of 90 μg/kg of rFVIIa was done three times at 2 h intervals. *POD* post-operative day

normal response to ADP stimulation (Fig. 3B). These results suggest that transfused platelets could support primary hemostatic plug formation during and after surgery. However, it should be also mentioned that the increment of αIIbβ3-positive platelets was only 17% of predicted increase of platelet count after platelet transfusion,

Table 1 Reported mutations in GT patients with alloantibodies

Age and sex	Type	Mutations	Gene	αIIbβ3-Ab	HLA-Ab	
14, F	I	IVS15(+1)G > A (premature termination), homo	ITGA2B	Pos	Unknown	Martin et al. [4]
18, F	I	IVS2(−2)A > G (premature termination), homo	ITGB3	Pos	Unknown	Male et al. [10]
55, M	I	IVS15(+1)G > A (premature termination), homo	ITGA2B	Pos	Unknown	Dargaud et al. [11]
Unknown	I	Exon 3 premature termination, homo	ITGB3	Pos	Neg	Santoro et al. [9]
Unknown[a]	I	1801T > C (C575R), homo	ITGB3	Pos	Pos	Santoro et al. [9]
M	I	1413C > G (Y471X)/1882C > T (R628X), compound hetero	ITGA2B	Pos	Neg	Nurden et al. [12]
59, M	I	892C > T (Q272X), homo	ITGB3	Pos	Pos	Our case

[a] Developed antibodies after massive (160 units) platelet transfusions

suggesting that the transfused platelets were rapidly cleared by anti-αIIbβ3 antibodies as anticipated.

Effectiveness of rFVIIa for GT with anti-αIIbβ3 antibodies is first described by Tengborn and Petruson [5], and international survey confirms it [6]. Although the precise mechanism of action of rFVIIa on GT platelets is largely unknown, impairment of thrombin generation capacity in GT platelets has been demonstrated. Experimental evidences suggest that high-dose rFVIIa can bind to activated platelet surface, and promote thrombin generation via direct activation of FX to FXa, which is sufficient to convert fibrinogen to fibrin [15]. Despite the lack of αIIbβ3, GT platelets have been shown to agglutinate in the presence of fibrin, particularly polymeric fibrin via unidentified receptors on platelet surface [16]. Although we could not assess the efficiency of rFVIIa in our case because platelet transfusion was used simultaneously, the fact that in spite of poor increment of transfused platelets bleeding in the surgery was minimal suggests the effectiveness of rFVIIa.

In conclusion, we found a novel β3 mutation, leading a premature termination of translation, in a GT patient with anti-αIIbβ3 antibodies. We could also assess the impact of anti-αIIbβ3 antibodies by monitoring the survival and function of transfused platelets in surgery.

Acknowledgments This work was supported in part by Grant-in Aid for Scientific Research from the Ministry of Education, Culture, Sports, Science and Technology in Japan, from the Ministry of Health, Labor and Welfare in Japan; and "Academic Frontier" Project in Japan.

Conflict of interest There are no conflicts of interest.

References

1. Tomiyama Y. Glanzmann thrombasthenia: integrin αIIbβ3 deficiency. Int J Hematol. 2000;72:448–54.
2. Gruel Y, Brojer E, Nugent DJ, Kunicki TJ. Further characterization of the thrombasthenia-related idiotype OG. Antiidiotype defines a novel epitope(s) shared by fibrinogen B beta chain, vitronectin, and von Willebrand factor and required for binding to β3. J Exp Med. 1994;180:2259–67.
3. Ito K, Yoshida H, Hatoyama H, Matsumoto H, Ban C, Mori T, et al. Antibody removal therapy used successfully at delivery of a pregnant patient with Glanzmann's thrombasthenia and multiple anti-platelet antibodies. Vox Sang. 1991;61:40–6.
4. Martin I, Kriaa F, Proulle V, Guillet B, Kaplan C, D'Oiron R, et al. Protein A Sepharose immunoadsorption can restore the efficacy of platelet concentrates in patients with Glanzmann's thrombasthenia and anti-glycoprotein IIb–IIIa antibodies. Br J Haematol. 2002;119:991–7.
5. Tengborn L, Petruson B. A patient with Glanzmann thrombasthenia and epistaxis successfully treated with recombinant factor VIIa. Thromb Hemost. 1996;75:981–2.
6. Poon MC, D'Oiron R, Von Depka M, Khair K, Négrier C, Karafoulidou A, et al. International Data Collection on Recombinant Factor VIIa and Congenital Platelet Disorders Study Group. Prophylactic and therapeutic recombinant factor VIIa administration to patients with Glanzmann's thrombasthenia: results of an international survey. J Thromb Haemost. 2004;2:1096–103.
7. Kosugi S, Tomiyama Y, Honda S, Kato H, Kiyoi T, Kashiwagi H, et al. Platelet-associated anti-GPIIb-IIIa autoantibodies in chronic immune thrombocytopenic purpura recognizing epitopes close to the ligand-binding site of glycoprotein (GP) IIb. Blood. 2001;98:1819–27.
8. Bellucci S, Caen J. Molecular basis of Glanzmann's Thrombasthenia and current strategies in treatment. Blood Rev. 2002;16:193–202.
9. Santoro C, Rago A, Biondo F, Conti L, Pulcinelli F, Laurenti L, et al. Prevalence of allo-immunization anti-HLA and anti-integrin αIIbβ3 in Glanzmann Thrombasthenia patients. Haemophilia. 2010;16:805–12.
10. Male C, Koren D, Eichelberger B, Kaufmann K, Panzer S. Monitoring survival and function of transfused platelets in Glanzmann thrombasthenia by flow cytometry and thrombelastography. Vox Sang. 2006;91:174–7.
11. Dargaud Y, Bordet JC, Trzeciak MC, Vinciguerra C, Negrier C. A case of Glanzmann's thrombasthenia successfully treated with recombinant factor VIIa during a surgical procedure: observation on the monitoring and the mechanism of this drug. Haemotologica. 2006;91:58–61.
12. Nurden AT, Kunicki T, Nurden P, Fiore M, Martins N, Heilig R, et al. Mutation analysis for a patient with Glanzmann Thrombasthenia who produced a landmark alloantibody to the αIIbβ3 integrin. J Thromb Haemost. 2010;8:1866–8.
13. Nurden A, Combrie R, Nurden P. Detection of transfused platelets in a patient with Glanzmann thrombasthenia. Thromb Haemost. 2002;87:543–4.

14. Shattil SJ, Cunningham M, Hoxie JA. Detection of activated platelets in whole blood using activation-dependent monoclonal antibodies and flow cytometry. Blood. 1987;70:307–15.
15. Monroe DM, Hoffman M, Oliver JA, Roberts HR. Platelet activity of high-dose factor VIIa is independent of tissue factor. Br J Haematol. 1997;99:542–7.
16. Poon MC. Clinical use of recombinant human activated factor VII (rFVIIa) in the prevention and treatment of bleeding episodes in patients with Glanzmann's thrombasthenia. Vasc Health Risk Manag. 2007;3:655.

THE JOURNAL OF BIOLOGICAL CHEMISTRY VOL. 285, NO. 32, pp. 24494–24507, August 6, 2010

Essential *in Vivo* Roles of the C-type Lectin Receptor CLEC-2

EMBRYONIC/NEONATAL LETHALITY OF CLEC-2-DEFICIENT MICE BY BLOOD/LYMPHATIC MISCONNECTIONS AND IMPAIRED THROMBUS FORMATION OF CLEC-2-DEFICIENT PLATELETS[*S]◆

Received for publication, April 5, 2010, and in revised form, May 11, 2010 Published, JBC Papers in Press, June 4, 2010, DOI 10.1074/jbc.M110.130575

Katsue Suzuki-Inoue,[a1,2] Osamu Inoue,[a1,3] Guo Ding,[b] Satoshi Nishimura,[c,d,e] Kazuya Hokamura,[f] Koji Eto,[g] Hirokazu Kashiwagi,[h] Yoshiaki Tomiyama,[i] Yutaka Yatomi,[j] Kazuo Umemura,[f] Yonchol Shin,[k] Masanori Hirashima,[b] and Yukio Ozaki[a]

From the [a]Department of Clinical and Laboratory Medicine, Faculty of Medicine, University of Yamanashi, 1110 Shimokato, Chuo, Yamanashi 409-3898, the [b]Division of Vascular Biology, Department of Physiology and Cell Biology, Kobe University Graduate School of Medicine, 7-5-1 Kusunoki-cho, Chuo-ku, Kobe, Hyogo 650-0017, the Departments of [c]Cardiovascular Medicine and [j]Laboratory Medicine, Graduate School of Medicine, and [d]Translational Systems Biology and Medicine Initiative, The University of Tokyo and [e]PREST, Japan Science and Technology Agency, 7-3-1 Hongo, Bunkyo-ku, Tokyo 113-8655, the [f]Department of Pharmacology, Hamamatsu University School of Medicine, 1-20-1 Handayama, Hamamatsu-shi, Sizuoka 431-3192, [g]The Stem Cell Bank, Center for Stem Cell Biology and Regenerative Medicine, The Institute of Medical Science, The University of Tokyo, 4-6-1 Shirokanedai, Minato-ku, Tokyo 108-8639, the [h]Department of Haematology and Oncology, Graduate School of Medicine C9, Osaka University, 2-2 Yamadaoka, Suita, Osaka 565-0871, the [i]Department of Blood Transfusion, Osaka University Hospital, 2-15 Yamadaoka, Suita, Osaka 565-0879, and the [k]Department of Applied Chemistry, Faculty of Engineering, Kogakuin University, 2665-1 Nakano, Hachioji, Tokyo 192-0015, Japan

CLEC-2 has been described recently as playing crucial roles in thrombosis/hemostasis, tumor metastasis, and lymphangiogenesis. The snake venom rhodocytin is known as a strong platelet activator, and we have shown that this effect is mediated by CLEC-2 (Suzuki-Inoue, K., Fuller, G. L., García, A., Eble, J. A., Pöhlmann, S., Inoue, O., Gartner, T. K., Hughan, S. C., Pearce, A. C., Laing, G. D., Theakston, R. D., Schweighoffer, E., Zitzmann, N., Morita, T., Tybulewicz, V. L., Ozaki, Y., and Watson, S. P. (2006) *Blood* 107, 542–549). Podoplanin, which is expressed on the surface of tumor cells, is an endogenous ligand for CLEC-2 and facilitates tumor metastasis by inducing platelet aggregation. Mice deficient in podoplanin, which is also expressed on the surface of lymphatic endothelial cells, show abnormal patterns of lymphatic vessel formation. In this study, we report on the generation and phenotype of CLEC-2-deficient mice. These mice are lethal at the embryonic/neonatal stages associated with disorganized and blood-filled lymphatic vessels and severe edema. Moreover, by transplantation of fetal liver cells from *Clec-2*$^{-/-}$ or *Clec-2*$^{+/+}$ embryos, we were able to demonstrate that CLEC-2 is involved in thrombus stabilization *in vitro* and *in vivo*, possibly through homophilic interactions without apparent increase in bleeding tendency. We propose that CLEC-2 could be an ideal novel target protein for an anti-platelet drug, which inhibits pathological thrombus formation but not physiological hemostasis.

The C-type lectin receptors are now established as multifunctional molecules in the field of cell adhesion, endocytosis, and pathogen recognition (1, 2). CLEC-2 (C-type lectin-like receptor-2) has been described recently as playing crucial roles in thrombosis/hemostasis, tumor metastasis, and lymphangiogenesis based on the following findings, reported mainly by us. (i) The snake venom rhodocytin is known as a strong platelet activator, and this effect has been shown to be mediated by CLEC-2 (3). (ii) Podoplanin is an endogenous ligand for CLEC-2, is expressed on the surface of tumor cells, and facilitates tumor metastasis by inducing platelet aggregation (4, 5). (iii) Mice deficient in podoplanin, which is expressed on the surface of lymphatic endothelial cells, show defects in lymphatic vessel pattern formation (6).

We have also reported that an anti-podoplanin antibody that blocks CLEC-2/podoplanin interaction inhibits tumor metastasis in an experimental lung metastasis model in mice, suggesting that CLEC-2 facilitates tumor metastasis through association with podoplanin (7). However, podoplanin is also expressed on the surface of lymphatic endothelial cells, kidney podocytes, and type I alveolar cells (8, 9). We and others found previously that podoplanin on the surface of lymphatic endothelial cells also induces platelet aggregation (4, 5). The physiological significance of this receptor/ligand interaction remains to be elucidated because lymphatic endothelial cells are not in direct contact with platelets under physiological conditions. However, it may be of great importance during organ development or under pathological conditions. It was reported previously that podoplanin-deficient mice have defects in lymphatic vessel pattern formation (6). The intracellular signaling molecules Syk (spleen tyrosine kinase) and SLP-76 (SH2 domain-containing leukocyte protein of 76 kDa) in platelets are requisites for rhodocytin-induced platelet activation mediated through CLEC-2 (3) and regulate blood and lymphatic vascular

* This work was supported in part by a grant-in-aid for scientific research from the Ministry of Education, Culture, Sports, Science, and Technology of Japan and by the Ministry of Health, Labor, and Welfare of Japan.
◆ This article was selected as a Paper of the Week.
[S] The on-line version of this article (available at http://www.jbc.org) contains supplemental Figs. 1–3, Table 1, and Videos 1 and 2.
[1] Both authors contributed equally to this work.
[2] To whom correspondence may be addressed. Tel.: 81-55-273-9884; Fax: 81-55-273-6713; E-mail: katsuei@yamanashi.ac.jp.
[3] To whom correspondence may be addressed. E-mail: oinoue@yamanashi.ac.jp.

separation, although these signaling molecules are not detected in the endothelium (10). This finding implies that Syk and SLP-76 work by way of blood cells. Moreover, blood/lymphatic misconnection is observed in mice deficient in endothelial cell *O*-glycan (11), the presence of which is required for podoplanin-induced platelet aggregation (4). Taken together, these findings lead to a hypothesis that podoplanin-induced platelet activation through CLEC-2 may regulate proper formation of lymphatic vessels. To address this issue, the generation of CLEC-2-deficient mice has been ardently awaited.

The powerful platelet-activating ability of CLEC-2 and its relatively specific expression in platelets and megakaryocytes imply that CLEC-2 also plays an important role in thrombosis and hemostasis. However, neither podoplanin nor rhodocytin can stimulate platelets within blood vessels. In addition, CLEC-2 ligands that play a role in thrombosis and hemostasis are not known. Therefore, the generation of CLEC-2-deficient mice has been awaited to reveal a role for CLEC-2 in thrombosis and hemostasis.

In this study, for the first time, we report on the generation and phenotype of CLEC-2-deficient mice. These mice are lethal at the embryonic/neonatal stage with blood/lymphatic misconnections. Moreover, by transplantation of fetal liver cells from *Clec-2*$^{-/-}$ or *Clec-2*$^{+/+}$ embryos, we were able to demonstrate that CLEC-2 is involved in thrombus stabilization, possibly through homophilic interactions.

EXPERIMENTAL PROCEDURES

Generation of Mice—A targeting vector to generate CLEC-2-deficient mice was designed so that part of exon 1 flanked by two *loxP* sites could be deleted by expression of Cre protein (supplemental Fig. 1*A*). ES[4] cells from C57BL/6 mice were transfected with this targeting vector, G418-resistant clones were screened by PCR, and positive clones were subjected to Southern blot analysis using a 3′-probe (supplemental Fig. 1, *A* and *B*). Nine ES clones were obtained containing the appropriately targeted disrupted allele and injected into blastocysts. Germ line transmission confirmed by PCR and Southern blotting was obtained in six independent ES cell clones (hereafter referred to as *Clec-2*$^{flox/+}$). We crossed a *Clec-2*$^{flox/+}$ mouse with a mouse that systemically expresses Cre recombinase to generate *Clec-2*$^{+/-}$ mice. The heterozygous mice were phenotypically normal and were bred to obtain homozygous mice for the allele containing the disrupted exon 1 of the *Clec-2* gene. For analysis of genotypes of *Clec-2* floxed mice, DNA was subjected to 30 cycles of amplification, with each cycle consisting of 20 s at 94 °C and 7 min at 62 °C, followed by an extension of 10 min at 74 °C on a thermal cycler using the long F2 and exon R primers, and PCR products were separated by 7.5% acrylamide gels (supplemental Fig. 1*A*). The WT allele gave a 229-bp band, whereas the floxed allele gave a 269-bp band by primers b and c (supplemental Fig. 1*C*). For analysis of genotypes of CLEC-2 null mice, DNA was subjected to 30 cycles of amplification, with each cycle consisting of 20 s at 94 °C and 7 min at 60 °C, followed by an extension of 10 min at 74 °C on a thermal cycler using the long F1 and exon R (733-bp band) primers for the WT allele and the neo R and long F2 (871-bp band) primers for the deleted allele, and PCR products were separated on 0.8% agarose gels (supplemental Fig. 1, *A* and *D*).

Lymphangiography—To visualize functional lymphatic vessels, FITC-dextran (Sigma; 2000 kDa; 8 mg/ml in PBS) was injected subcutaneously into the back of the embryonic forelimb. Lymphatic flow carrying FITC-dextran in embryos was analyzed by fluorescence microscopy (12).

Microscopy—Embryos were photographed at autopsy. For routine histology, embryos were fixed in 3.7% formalin and embedded in paraffin. Sections were stained with hematoxylin and eosin.

For immunohistochemistry, deparaffinized sections were stained with rabbit anti-mouse LYVE-1 antibody (Abcam Inc.) using Simplestain® mouse MAX-PO (rabbit; Nichirei Corp.) according to the manufacturer's instruction. For confocal microscopy, embryos (E17.5) were fixed overnight in 4% paraformaldehyde at room temperature; washed; and cryoprotected with 10% sucrose for 2 h, 20% sucrose for 2 h, and 40% sucrose overnight. The samples were then mounted in OCT (optimal cutting temperature) compound (Sakura Finetek). Cryosections (~10 μm) were incubated overnight at 4 °C with biotin-conjugated goat anti-mouse LYVE-1 antibody (R&D Systems), rat anti-mouse PECAM-1 (platelet endothelial cell adhesion molecule-1) monoclonal antibody (clone MEC13.3, BD Biosciences), and Cy3-conjugated anti-α-smooth muscle actin monoclonal antibody (clone 1A4, Sigma); developed with Cy5-labeled streptavidin (Invitrogen) and Alexa Fluor 488-conjugated donkey anti-rat IgG (Invitrogen) for 2 h at room temperature; and mounted with ProLong Gold mounting medium. The samples were analyzed by confocal laser-scanning microscopy using an Olympus FV-1000 microscope.

For immunohistochemical analysis of embryonic back skin, whole embryos were dissected between E14.5 and E17.5 and fixed overnight at 4 °C in 4% paraformaldehyde/PBS. The back skin was peeled off and further fixed overnight at 4 °C in 4% paraformaldehyde/PBS. Tissues were washed twice with PBS containing 0.2% Triton X-100 (PBS/T) at 4 °C for 30 min; blocked in PBS/T containing 1% bovine serum albumin at room temperature for 1 h; and stained overnight with American hamster anti-mouse PECAM-1 (clone 2H8, Chemicon), rabbit anti-mouse LYVE-1 (RELIATech), and rat anti-mouse TER-119 (clone TER-119, BD Biosciences) antibodies in blocking solution at 4 °C. Tissues were washed with PBS/T for 30 min three times at 4 °C and twice at room temperature, followed by overnight staining with Cy3-conjugated anti-American hamster IgG and Cy5-conjugated anti-rat IgG (Jackson ImmunoResearch Laboratories) or Alexa Fluor 488-conjugated anti-rabbit IgG (Invitrogen) in blocking solution at 4 °C. Tissues were washed with PBS/T for 30 min three times at 4 °C and twice at room temperature. The back skin was flat-mounted on slide glasses in ProLong Antifade (Invitrogen). Confocal microscopy was carried out on an Olympus FV-1000 microscope.

[4] The abbreviations used are: ES, embryonic stem; WT, wild-type; FITC, fluorescein isothiocyanate; E, embryonic day; PBS, phosphate-buffered saline; GP, glycoprotein; PE, phycoerythrin; vWF, von Willebrand factor; BSA, bovine serum albumin; TRITC, tetramethylrhodamine isothiocyanate; PPACK, D-phenylalanyl-L-prolyl-L-arginine chloromethyl ketone; FcR, Fc receptor.

Fetal Liver Transplantation—CLEC-2-deficient irradiated chimeric mice were generated as follows. Seven- to ten-week-old C57BL/6 male mice that had been kept on acidified water for one week and then on 0.017% enrofloxacin in water for 3 days were given two irradiations of 500 rads from a ^{60}Co source 3 h apart (13). The mice were then rescued by intravenous injection of 1.0×10^6 fetal liver cells from *Clec-2*$^{-/-}$ or control embryos at E13.5. The reconstituted mice were kept on 0.017% enrofloxacin in water for 3 weeks following irradiation and were used for experiments no fewer than 7 weeks following irradiation.

Platelet Preparation—Mice were killed with diethyl ether, and blood was drawn by postcava puncture and taken into 100 μl of acid/citrate/dextrose. Washed murine platelets were obtained by centrifugation as described previously using prostacyclin to prevent activation during the isolation procedure (14). Washed platelets were resuspended in modified Tyrode's buffer (14) at the indicated cell densities.

Generation of Rabbit anti-Mouse CLEC-2 Antibody—The recombinant extracellular domain of mouse CLEC-2 expressed as a dimeric rabbit immunoglobulin Fc domain fusion protein (mCLEC-2-rFc2) was generated as described previously (4). A purified polyclonal antibody specific for mouse CLEC-2 was purified by protein A-Sepharose (GE Healthcare) from the serum of a Japanese White rabbit after six immunizations with mCLEC-2-rFc2.

Western Blotting—Western blotting was performed as described previously (14). Briefly, washed murine platelets (2.0×10^8/ml) were dissolved in SDS sample buffer, separated by 4–12% SDS-PAGE, electrotransferred, and Western-blotted with anti-mouse CLEC-2 antibody.

Platelet Aggregation—Rhodocytin was purified as described previously (15). Poly(PHG), a specific GPVI agonist, was generated as described previously (16). 300 μl of washed platelets (2.0×10^8/ml) from CLEC-2 or WT chimeras was used for aggregation studies. The washed platelets were stimulated by rhodocytin (20 nM), collagen (1 μg/μl; Nycomed), U46619 (0.5 μM; Merck), ADP (5 μM; MC Medical), and PAR-4 (50 μM; Sigma), and platelet aggregation was monitored by light transmission using a Born aggregometer (PA-100, Kowa) with high speed stirring (1200 rpm) at 37 °C for 10 min.

Flow Cytometry—Whole blood drawn from mice as described above was diluted 15-fold using modified Tyrode's buffer. 25 μl of the diluted whole blood was incubated with Cy2-labeled anti-mouse CLEC-2, Cy2-labeled control rabbit IgG, PE-labeled control rat IgG (Emfret Analytics), FITC-labeled control rat IgG (Emfret Analytics), FITC-labeled anti-mouse GPVI (clone JAQ-1, Emfret Analytics), FITC-labeled anti-mouse integrin αIIb (Emfret Analytics), PE-labeled anti-mouse GPIbα (Emfret Analytics), FITC-labeled anti-mouse PECAM-1 (BD Biosciences), PE-labeled anti-mouse integrin α2 (clone HMα2, BD Biosciences), FITC-labeled control hamster IgG (Serotec), and FITC-labeled integrin β1 (Serotec) antibodies for 15 min at room temperature. For analysis of activated integrin αIIbβ3, 25 μl of diluted whole blood was stimulated with the indicated platelet agonists (20 nM rhodocytin, 20 μg/ml poly(PHG), 50 μg/ml collagen, 50 μM U46619, 40 μM ADP, and 100 μM PAR-4) for 5 min at room temperature, followed by the addition of anti-activated mouse integrin αIIbβ3 (clone Jon-A, Emfret Analytics) for 5 min at room temperature. For analysis of CD62P expression, 25 μl of washed platelets (5×10^7/ml) was used. Reactions were terminated by the addition of 400 μl of PBS, and the samples were then analyzed using a FACScan (BD Biosciences) and a CellQuest software (BD Biosciences). For detection of soluble mCLEC-2-rFc2 binding to platelets, WT or CLEC-2-deficient platelets (3×10^8/ml) were stimulated with or without 50 μM PAR-4 peptides for 5 min under non-stirring conditions. They were then incubated with 50 μg/ml recombinant mCLEC-2-rFc2 or rFc2 for 20 min. After washing with modified Tyrode's buffer, these cells were resuspended with 100 μl of PBS and stained with 2 μl of FITC-labeled anti-rabbit IgG (BD Biosciences) for 15 min. Stained cells were analyzed immediately using a FACScan and CellQuest software. Where indicated, quantification of the soluble protein binding was performed using median fluorescence intensity, and the data were expressed as the means ± S.E.

Measurement of Serotonin Release—Washed platelets (3×10^8/ml) from WT or CLEC-2 chimeras were stimulated with or without 20 nM rhodocytin, 20 μg/ml poly(PHG), or 50 μg/ml collagen for 5 min under non-stirring conditions. After spinning down the platelets, the serotonin concentration of 15 μl of the supernatant was measured using a 5-hydroxytryptamine enzyme-linked immunosorbent assay kit (DLD Diagnostika GmbH) according to the manufacturer's instructions.

Platelet Adhesion Assay—Coverslips were coated overnight at 4 °C with 50 μg/ml laminin, 50 μg/ml collagen, 200 μg/ml fibrinogen, 100 μg/ml vWF, 250 μg/ml rFc2, or 250 μg/ml mCLEC-2-rFc2. After washing twice with PBS, the coverslips were blocked with 1% fatty acid-free purified BSA in PBS for 2 h at room temperature and then rinsed with modified Tyrode's buffer. BSA-coated coverslips were prepared as a negative control. Washed murine platelets (3.0×10^7/ml) were seeded on the coverslips for 30 min at room temperature in the presence or absence of 10 μM ADP. After removal of unbound platelets, coverslips were washed with modified Tyrode's buffer, and adherent platelets were then fixed in 3% paraformaldehyde for 30 min at room temperature, permeabilized with 0.3% Triton X-100 for 5 min, and stained with TRITC-conjugated phalloidin for 2 h as described previously (17). Platelets were visualized using an inverted fluorescence microscope (IX71, Olympus) equipped with a 100×/1.30 objective lens, a monochromatic light source, and a DP-70 digital camera (Olympus). At least six images from two independent experiments were chosen at random per experiment and analyzed by two individuals, one of whom performed the analysis under blind conditions. Adherent platelets were counted (0.006 mm^2/image), and the platelet surface area was analyzed using NIH Image for Macintosh. Statistical significance was evaluated by Student's *t* test. In each case, p values <0.05 were taken as the minimum to indicate statistical significance.

Flow Adhesion Assay—Whole blood from WT or CLEC-2 chimeras was collected into a syringe and anticoagulated with 40 μM PPACK and 5 units/ml heparin. Capillary tubes (0.3 × 1.2 mm, 50 mm long) were coated overnight at 4 °C with 50 μg/ml collagen. Capillaries were washed and blocked with PBS containing 2% BSA for 2 h at room temperature. They were

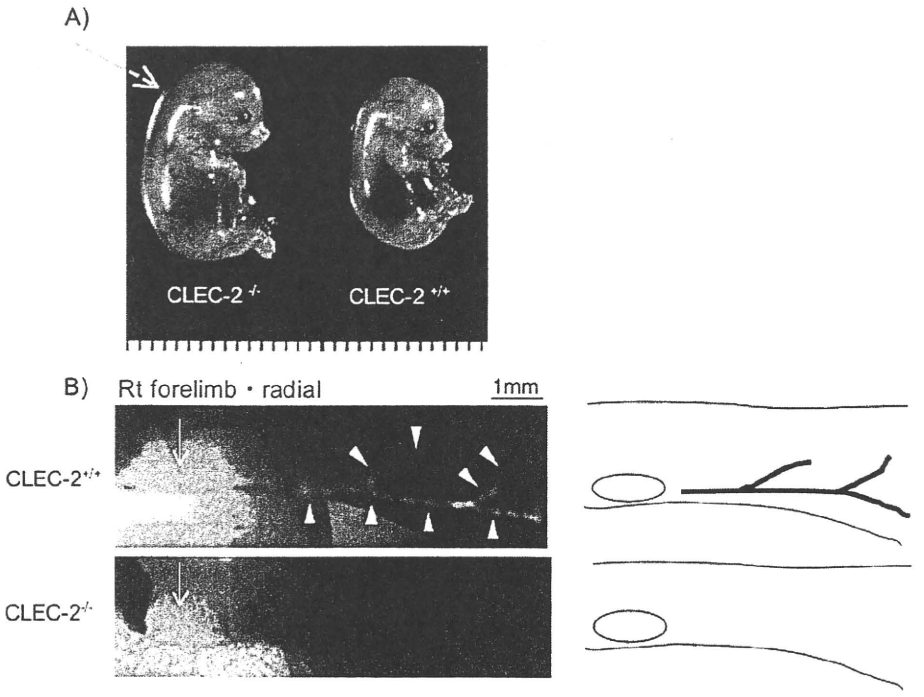

FIGURE 1. **Lymphatic function is impaired in *Clec-2*$^{-/-}$ embryos.** *A*, lateral views of E15.5 *Clec-2*$^{-/-}$ (*left*) and *Clec-2*$^{+/+}$ (*right*) embryos. Back edema in the *Clec-2*$^{-/-}$ embryo is indicated by the *arrow*. *B*, lymphangiography by injection of FITC-dextran into the forelimbs of *Clec-2*$^{+/+}$ (*upper panel*) and *Clec-2*$^{-/-}$ (*lower panel*) embryos at E17.5. Injection sites on the forelimbs are indicated by the *arrows*. The *arrowheads* indicate visualized collecting lymphatic vessels in the *Clec-2*$^{+/+}$ embryo. The *schematics* on the right illustrate the visualized collecting lymphatic vessel in *Clec-2*$^{+/+}$ mice (*upper panel*) and injection sites in *Clec-2*$^{+/+}$ (*upper panel*) and *Clec-2*$^{-/-}$ (*lower panel*) embryos (*arrow*). *Rt*, right.

then rinsed with modified Tyrode's buffer supplemented with 2 mM $CaCl_2$ and 1 unit/ml heparin and connected to a syringe filled with the anticoagulated blood that had been pretreated with 5 μM 3,3′-dihexyloxacarbocyanine iodide for 30 min. Blood was perfused into capillaries at 2000 s^{-1}, and adherent platelets were visualized using a fluorescence video microscope (IX71). Where indicated, 10 μM ADP was co-infused with the anticoagulated blood shortly before entrance into the capillary tubes. Movie data were converted into sequential photo images. For measurement of thrombus volume, capillaries with thrombus were visualized using an Olympus FV-1000 confocal microscope. The data were analyzed using FluoView software (Olympus), and thrombus volume was expressed as integrated fluorescence intensity. Platelet concentrations were counted 1 week before the experiments so that platelet counts were same between WT and CLEC-2 chimeras.

Intravital Microscopy and Thrombus Formation—To visually analyze thrombus formation in the microcirculation of the mesentery in living animals, we used *in vivo* laser injury and visualization techniques developed through modification of conventional methods (18, 19). Male mice were anesthetized by injection with urethane (1.5 g/kg), and a small incision was made so that the mesentery could be observed without being exteriorized. FITC-dextran (5 mg/kg of body weight) was injected into mice to visualize cell dynamics, whereas hematoporphyrin (1.8 mg/kg for capillary thrombi and 2.5 mg/kg for arterioles) was injected to produce reactive oxygen species upon laser irradiation. Blood cell dynamics and production of thrombi were visualized during laser excitation (488-nm wavelength, 30-milliwatt power). Sequential images were obtained for 20 s at 30 frames/s using a spinning-disk confocal microscope (CSU-X1, Yokogawa Electronics) and an electron-multiplying charged coupled device camera (iXon, Andor Technology). Platelet concentrations were counted 1 week before the experiments so that platelet counts were same between WT and CLEC-2 chimeras.

Tail Bleeding—Mice were anesthetized with 3.5% Sevoflurane and 0.5 liter/min O_2 through a face mask throughout the experiment. We laid each mouse on its stomach and arranged the tail horizontally with the tip hanging over the edge of the bench. We then cut off the tip of the tail (1 mm in length) with a sharp razor blade. The volume of blood lost during the 20-min experiment was measured. After surgical suture of the tail wound, we let the mice recover from anesthesia. Platelet concentrations were counted 1 week before the experiments so that platelet counts were same between WT and CLEC-2 chimeras.

Surface Plasmon Resonance Spectroscopy—The recombinant extracellular domain of human or mouse CLEC-2 expressed as a dimeric human or rabbit immunoglobulin Fc domain fusion protein (hCLEC-2-rFc2 and mCLEC-2-rFc2) was generated as described previously (4). A specific homophilic interaction between hCLEC-2-rFc2 or mCLEC-2-rFc2 was analyzed using a Biacore X system (Biacore AB, Uppsala, Sweden). Ligands ($\alpha v\beta 3$, $\alpha 2\beta 1$, CD62P, LIMP-II (lysosomal integral membrane protein-II), TSP-1, PEAR-1 (platelet endothelial aggregation receptor 1) (all purchased from R&D Systems), hCLEC-2-rFc2, and mCLEC-2-rFc2) were covalently coupled to a CM5 chip (Biacore AB) using an amine coupling kit (Biacore AB) according to the manufacturer's instructions (20). Regeneration of the protein-coated surfaces was achieved by running 10 μl of 10 mM HCl thorough the flow cell at 20 μl/min twice. A control surface was reacted with rFc2 and then blocked with ethanolamine. hCLEC-2-rFc2 or mCLEC-2-rFc2 in 10 mM HEPES, 0.15 M NaCl, 3 mM EDTA, and 0.005% Tween 20 (pH 7.4) (Biacore AB) at several concentrations was perfused over the control surface or an immobilized hCLEC-2-rFc2 or mCLEC-2-rFc2 surface at a flow rate of 20 μl/min at 25 °C, and the resonance changes were recorded. The response from the hCLEC-2-rFc2 or mCLEC-2-rFc2 surface was subtracted from that of the control surface. The dissociation constants (K_d) were determined using BIAevaluation software.

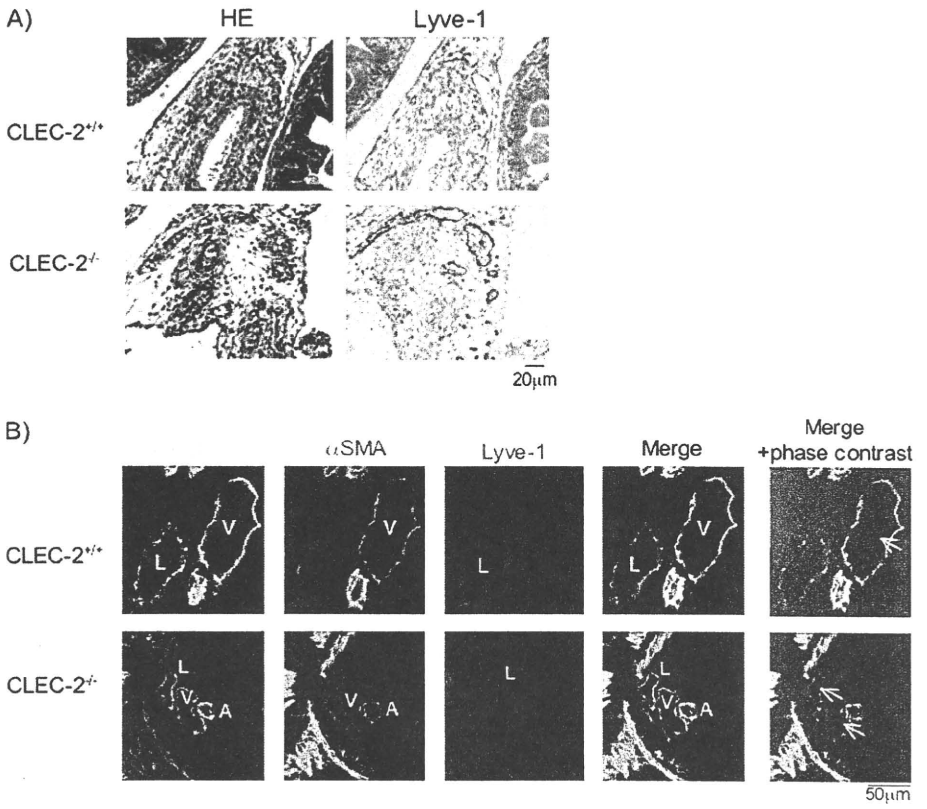

FIGURE 2. **Developing lymphatic circulation in mice lacking CLEC-2 communicates with the blood circulation.** *A*, mesenteric sections of E15.5 *Clec-2*$^{+/+}$ (*upper panels*) and *Clec-2*$^{-/-}$ (*lower panels*) embryos stained with hematoxylin and eosin (*HE*; *left panels*) and LYVE-1 (*right panels*). *B*, confocal images of intestinal cryosections of E17.5 *Clec-2*$^{+/+}$ (*upper panels*) and *Clec-2*$^{-/-}$ (*lower panels*) embryos with antibodies against PECAM-1, α-smooth muscle actin (*α-SMA*), and LYVE-1. *L*, lymphatic vessels; *V*, vein; *A*, arteries. The *arrows* indicate blood cells.

RESULTS

Generation of CLEC-2-deficient Mice—A targeting vector to generate CLEC-2-deficient mice was designed so that part of exon 1 flanked by two *loxP* sites could be deleted by expression of Cre protein (supplemental Fig. 1*A*). Nine ES clones were obtained, which contained the appropriately targeted allele, and were injected into C57BL/6 blastocysts. Southern blot analysis confirmed the presence of the targeted locus (supplemental Fig. 1, *A* and *B*). Germ line transmission was obtained from six independent ES cell clones (hereafter referred to as *Clec-2*$^{flox/+}$). We crossed a *Clec-2*$^{flox/+}$ mouse with a mouse that systemically expresses Cre recombinase to generate *Clec-2*$^{+/-}$ mice. Germ line transmission was confirmed by PCR and Southern blotting. The heterozygous mice were phenotypically normal and were bred to obtain homozygous mice for the allele containing the disrupted exon 1 of the *Clec-2* gene.

Genotype analysis of embryos from heterozygous intercrosses at E13.5 showed the expected numbers of *Clec-2*$^{-/-}$ embryos. However, the percentage of the knock-out embryos dropped to less than expected at E15.5 (supplemental Table 1). We analyzed genotypes of 326 newborn mice and found that the percentage of the knock-out mice was only 9.8% (supplemental Table 1). Moreover, most of the *Clec-2*$^{-/-}$ pups died shortly after birth, and only two *Clec-2*$^{-/-}$ mice of 326 mice survived after 8 weeks of age, suggesting that *Clec-2*$^{-/-}$ mice are lethal at the embryonic/neonatal stage. There were fewer heterozygotes than predicted by Mendelian inheritance (supplemental Table 1). We do not have any direct evidence to explain this phenomenon. It is plausible that the heterozygotes may also have some developmental abnormality related to lymphatic vessels that causes intrauterine death of some pups. This needs further investigation.

CLEC-2-deficient Mice Exhibit Disorganized Vasculature and Impaired Lymphatic Function—To investigate the cause of the embryonic or neonatal lethality of CLEC-2-deficient mice, we examined *Clec-2*$^{-/-}$ embryos. Cutaneous hemorrhagic appearance was the most striking phonotype observed in CLEC-2-lacking embryos (Fig. 1*A*), which was first noted at E12.5–E13.5. Edema was observed in the back skin in CLEC-2-deficient embryos (Fig. 1*A*, *arrow*), implying impaired lymphatic drainage. We assessed lymphatic function by infusing 2000-kDa FITC-dextran into embryonic limbs. Lymphangiography showed normal collecting lymphatic vessels immediately after dye infusion in WT mice at E17.5 (Fig. 1*B*, *upper inlet*, *arrow*), whereas dye uptake was not found even 10 min after injection (*lower inlet*), suggesting functional defects in lymphatic drainage of *Clec-2*$^{-/-}$ embryos.

Histological analysis of the mesentery of CLEC-2-deficient embryos revealed that peripheral blood cells were present within thin-walled vessels that stained for LYVE-1, a molecular marker of lymphatic endothelial cells, whereas there were no blood cells in LYVE-1-positive vessels in WT embryos (Fig. 2*A*). Triple fluorescence staining for smooth muscle actin and PECAM-1 (but not for LYVE-1) revealed that only blood vessels, but not lymphatic vessels, contained blood cells in WT embryos (Fig. 2*B*). On the other hand, lymphatic vessels as well as blood vessels contained blood cells in CLEC-2-deficient embryos (Fig. 2*B*). These findings indicate that CLEC-2-deficient mice have blood-filled lymphatic vessels.

To investigate the network formation of blood and lymphatic vessels, we performed whole-mount triple fluorescence confocal microscopy of embryonic back skin using antibodies to PECAM-1, LYVE-1, and TER-119 (a molecular marker of erythrocytes). Triple staining revealed that the dilated lymphatic vessels in CLEC-2-deficient embryos contained erythrocytes, whereas those in WT embryos did not contain blood, further confirming the blood-filled lymphatic vessels in *Clec-2*$^{-/-}$ embryos. In CLEC-2-deficient embryos, lymphatic vessels